Cell

EphB-Mediated Degradation of the RhoA GEF Ephexin5 Relieves a Developmental Brake on Excitatory Synapse Formation

Seth S. Margolis,[1,3] John Salogiannis,[1,3] David M. Lipton,[1] Caleigh Mandel-Brehm,[1] Zachary P. Wills,[1] Alan R. Mardinly,[1] Linda Hu,[1] Paul L. Greer,[1] Jay B. Bikoff,[1] Hsin-Yi Henry Ho,[1] Michael J. Soskis,[1] Mustafa Sahin,[2] and Michael E. Greenberg[1,*]

[1]Department of Neurobiology, Harvard Medical School, 220 Longwood Avenue, Boston, MA 02115, USA
[2]F.M. Kirby Neurobiology Center, Departments of Neurology, Children's Hospital Boston, Harvard Medical School, Boston, MA 02115, USA
[3]These authors contributed equally to this work
*Correspondence: michael_greenberg@hms.harvard.edu
DOI 10.1016/j.cell.2010.09.038

SUMMARY

The mechanisms that promote excitatory synapse formation and maturation have been extensively studied. However, the molecular events that limit excitatory synapse development so that synapses form at the right time and place and in the correct numbers are less well understood. We have identified a RhoA guanine nucleotide exchange factor, Ephexin5, which negatively regulates excitatory synapse development until EphrinB binding to the EphB receptor tyrosine kinase triggers Ephexin5 phosphorylation, ubiquitination, and degradation. The degradation of Ephexin5 promotes EphB-dependent excitatory synapse development and is mediated by Ube3A, a ubiquitin ligase that is mutated in the human cognitive disorder Angelman syndrome and duplicated in some forms of Autism Spectrum Disorders (ASDs). These findings suggest that aberrant EphB/Ephexin5 signaling during the development of synapses may contribute to the abnormal cognitive function that occurs in Angelman syndrome and, possibly, ASDs.

INTRODUCTION

A crucial early step in the formation of excitatory synapses is the physical interaction between the developing presynaptic specialization and the postsynaptic dendrite (Jontes et al., 2000; Ziv and Smith, 1996). This step in excitatory synapse development is thought to be mediated by cell surface membrane proteins expressed by the developing axon and dendrite and appears to be independent of the release of the excitatory neurotransmitter glutamate (reviewed in Dalva et al., 2007). Several recent studies have revealed an important role for Ephrin cell surface-associated ligands and Eph receptor tyrosine kinases in this early cell-cell contact phase that is critical for excitatory synapse formation (Dalva et al., 2000; Ethell et al., 2001; Henkemeyer et al., 2003; Kayser et al., 2006; Kayser et al., 2008; Lai and Ip, 2009; Murai et al., 2003). Ephs can be divided into two classes, EphA and EphB, based on their ability to bind the ligands EphrinA and EphrinB, respectively (reviewed in Flanagan and Vanderhaeghen, 1998). EphBs are expressed postsynaptically on the surface of developing dendrites, while their cognate ligands, the EphrinBs, are expressed on both the developing axon and dendrite (Grunwald et al., 2004; Grunwald et al., 2001; Lim et al., 2008). When an EphrinB encounters an EphB on the developing dendrite, EphB becomes autophosphorylated, thus increasing its catalytic kinase activity (reviewed in Flanagan and Vanderhaeghen, 1998). This leads to a cascade of signaling events including the activation of guanine nucleotide exchange factors (GEFs) Tiam, Kalirin, and Intersectin, culminating in actin cytoskeleton remodeling that is critical for excitatory synapse development (reviewed in Klein, 2009). Consistent with a role for EphBs in excitatory synapse development, EphB1/EphB2/EphB3 triple knockout mice have fewer mature excitatory synapses in vivo in the cortex, and hippocampus (Henkemeyer et al., 2003; Kayser et al., 2006). In addition, the disruption of EphB function postsynaptically in dissociated hippocampal neurons leads to defects in spine morphogenesis and a decrease in excitatory synapse number (Ethell et al., 2001; Kayser et al., 2006). Conversely, activation of EphBs in hippocampal neurons leads to an increase in the number of dendritic spines and functional excitatory synapses (Henkemeyer et al., 2003; Penzes et al., 2003).These findings indicate that EphBs are positive regulators of excitatory synapse development.

While there has been considerable progress in characterizing the mechanisms by which EphBs promote excitatory synapse development, it is not known if there are EphB-associated factors that restrict the timing and extent of excitatory synapse development. We hypothesized that neurons might have evolved mechanisms which act as checkpoints to restrict EphB-mediated synapse formation, and that the release from such synapse formation checkpoints might be required if synapses are to form at the correct time and place and in appropriate numbers.

We considered the possibility that likely candidates to mediate the EphB-dependent restriction of excitatory synapse formation might be regulators of RhoA, a small G protein that functions to

antagonize the effects of Rac (Tashiro et al., 2000). In previous studies we identified a RhoA GEF, Ephexin1 (E1), which interacts with EphA4 (Fu et al., 2007; Sahin et al., 2005; Shamah et al., 2001). E1 is phosphorylated by EphA4 and is required for the EphrinA-dependent retraction of axonal growth cones and dendritic spines (Fu et al., 2007; Sahin et al., 2005). While E1 does not appear to interact with EphB, E1 is a member of a family of five closely related GEFs. Of these GEFs, Ephexin5 (E5) (in addition to E1) is highly expressed in the nervous system. Therefore, we hypothesized that E5 might function to restrict the EphB-dependent development of excitatory synapses by activating RhoA.

In this study we report that EphB interacts with E5, that E5 suppresses excitatory synapse development by activating RhoA, and that this suppression is relieved by EphrinB activation of EphB during synapse development. Upon binding EphrinB, EphB catalyzes the tyrosine phosphorylation of E5 which triggers E5 degradation. We identify Ube3A as the ubiquitin ligase that mediates E5 degradation, thus allowing synapse formation to proceed. As *Ube3A* is mutated in Angelman syndrome and duplicated in some forms of Autism Spectrum Disorders (ASDs), these findings suggest a possible mechanism by which the mutation of Ube3A might lead to cognitive dysfunction (Jiang et al., 1998; Kishino et al., 1997). Specifically, we provide evidence that in the absence of Ube3A, the level of E5 is elevated and propose that this may lead to the enhanced suppression of EphB-mediated excitatory synapse formation, thereby contributing to Angelman syndrome.

RESULTS

Ephexin5 Interacts with EphB2

To identify mechanisms that restrict the ability of EphBs to promote an increase in excitatory synapse number, we searched for guanine nucleotide exchange factors (GEFs) that specifically activate RhoA signaling, are expressed in the same population of neurons that express EphB, are expressed at the same time during development as EphB, and interact with EphB. Structure-function studies of GEFs identified amino acid residues in the activation domain of Rho family GEFs that specifically identify the GEFs as activators of RhoA rather than Rac or Cdc42. Applying this criterion, fourteen GEFs were identified that specifically activate RhoA (Rossman et al., 2005). Of these GEFs we found by in situ hybridization that E5 has a similar expression pattern to EphB in the hippocampus (Figure 1A). These findings raised the possibility that E5 might mediate the effect of EphB on developing synapses.

We asked if E5 interacts physically with EphB. We transfected HEK293T (293) cells with plasmids encoding Myc-tagged E5, E1, or a vector control together with Flag-tagged EphB2 or EphA4 and asked if these proteins coimmunoprecipitate. Extracts were prepared from the transfected 293 cells and EphA4 or EphB2 immunoprecipitated with Flag antibodies. The immunoprecipitates were subjected to SDS polyacrylamide gel electrophoresis (SDS-PAGE) and blotted with anti-Myc antibody (α-Myc). We found that E5 coimmunoprecipitates with EphB2 but not with EphA4 (Figure 1B). The relatively weak E5 interaction with EphA4 is consistent with published experiments (Ogita

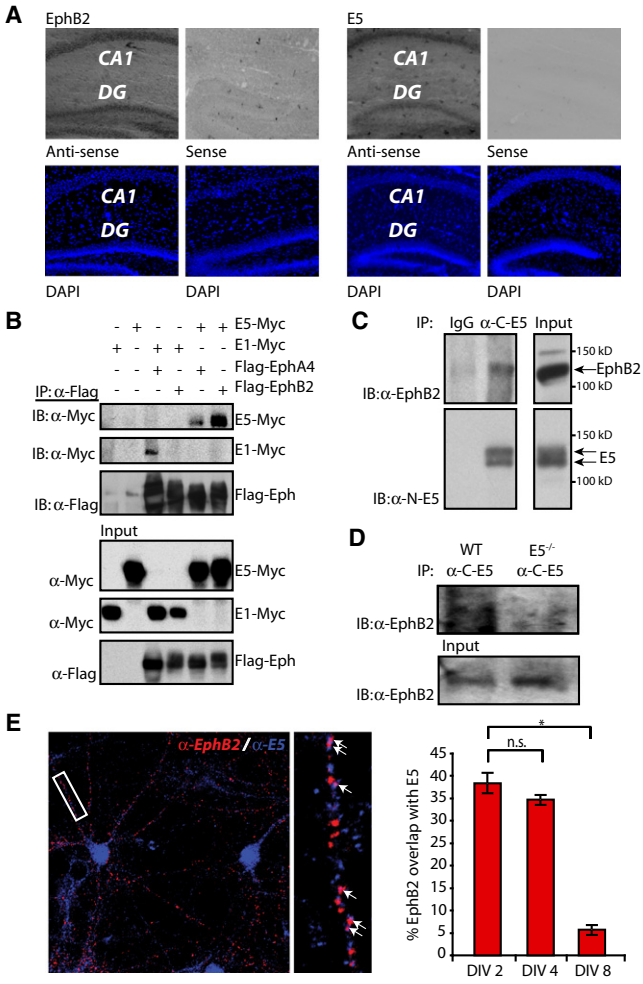

Figure 1. Ephexin5 Interacts with EphB2

(A) E5 and EphB2 are expressed in the CA1 region and dentate gyrus (DG) of the hippocampus at P12. Adjacent 14 μm mouse brain sections were stained for E5 or EphB2 using digoxigenin-labeled RNA probes to the antisense strand or sense strand as a control (top). Lower panels show nuclear staining with DAPI.

(B) Immunoprecipitation with α-Flag from 293 cell lysates previously transfected with various combinations of overexpressing plasmids containing E1-Myc, E5-Myc, Flag-EphB2, and/or Flag-EphA4, followed by immunoblotting with α-Myc or α-Flag. Input protein levels are shown (bottom).

(C) Immunoprecipitation of mouse cortical lysates with IgG or α-C-E5, followed by immunoblotting with α-EphB2 or α-N-E5 (left). Input protein levels are shown (right).

(D) Immunoprecipitation of WT or $E5^{-/-}$ mouse cortical culture lysates with α-C-E5 followed by immunoblotting with α-EphB2. Input EphB2 levels are shown (bottom).

(E) Dissociated rat hippocampal neurons were stained using α-N-E5 (Blue) and α-EphB2 (Red). A representative image of overlapped EphB2 and E5 is shown (left). White rectangle outlines magnified dendritic region (right) showing examples of EphB2/E5 colocalization (arrows). In three independent experiments, quantification of overlapped EphB2/E5 puncta was determined at DIV2, DIV4 and DIV8 and is represented as percent of EphB2 overlapped with E5 (right). Error bars ± SEM; *p < 0.05, nonsignificant (n.s.).

See also Figure S1.

et al., 2003). By contrast, E1 is coimmunoprecipitated by EphA4 but not EphB2 (Shamah et al., 2001). These findings suggest that E5 interacts preferentially with EphB2.

To extend this analysis we investigated whether EphB2 interacts with E5 in neurons. Neurons from embryonic day 16 (E16) mouse brains were lysed in RIPA buffer and the lysates incubated with affinity purified anti-C-terminal E5 (α-C-E5) or control (IgG) antibodies. The immunoprecipitates were then resolved by SDS-PAGE and immunoblotted with affinity purified anti-N-terminal E5 (α-N-E5) or EphB2 (α-EphB2) antibodies (Figure 1C). This analysis revealed that endogenous, neuronal EphB2 is immunoprecipitated by α-C-E5 but not IgG. Moreover, using lysates from cortical cultures of wild-type or E5 knockout mice (*E5*$^{-/-}$, see Figure S1 available online), we find that α-C-E5 immunoprecipitates EphB2 only from lysates when E5 is present (Figure 1D). Taken together, these findings suggest that EphB interacts with Ephexin5 in neurons.

As an independent means of assessing if EphB and E5 interact with one another, we used immunofluorescence microscopy to determine if these two proteins colocalize in neurons. Cultured mouse hippocampal neurons were transfected with a plasmid expressing green fluorescent protein (GFP). The GFP-expressing neurons were imaged and quantified for the colocalization of EphB2 and E5 puncta by staining with α-C-E5 and α-EphB2. This analysis revealed that EphB2 and E5 colocalize along dendrites (Figure 1E). We find that 40% of EphB staining overlaps with α-C-E5 staining early during the development of excitatory synapses. After eight days in vitro (DIV) the overlap of EphB with E5 within neuronal dendrites decreases to below the level that would be detected by random chance. This change suggests that EphB interacts with E5 early during development but that these two proteins may not interact later in development.

Ephexin5 Is a Guanine Nucleotide Exchange Factor that Activates RhoA

To determine if E5 activates RhoA, we transfected 293 cells with a control plasmid or a plasmid that drives the expression of Myc-tagged mouse E5. We prepared extracts from the transfected cells and incubated the extracts with a GST-fusion protein that includes the Rhotekin-Binding Domain (GST-RBD), a protein domain that selectively interacts with active (GTP-bound) but not inactive (GDP-bound) RhoA. Following SDS-PAGE of the proteins in the extract that bind to GST-RBD, RhoA binding to GST-RBD was measured by immunoblotting with α-RhoA antibodies. We found that cells expressing E5 exhibited higher levels of activated RhoA compared to cells transfected with a control plasmid, indicating that E5 activates RhoA (Figure 2A).

When a similar series of experiments were performed using a GST-fusion Pak-Binding Domain (GST-PBD) which specifically interacts with active forms of two other Rho GTPases, Rac1 and Cdc42, we found that E5 does not induce the binding of GST-PBD to Rac1 or Cdc42. In contrast, E1-expressing cells displayed enhanced binding of Rac1 and Cdc42 to GST-PBD. We conclude that E5 activates RhoA but not Rac1 or Cdc42 (Figure S2A).

To determine whether E5 activation of RhoA requires the GEF activity of E5, we generated a mutant form of E5 in which its GEF activity is impaired. To identify the residues required for Ephexin5 guanine nucleotide exchange activity we compared its Dbl-homology (DH) domain to the DH domain of other RhoA-specific GEFs (Snyder et al., 2002). We identified within the α5 helix of E5's DH domain three amino acids that are conserved in other GEFs that, like E5, activate RhoA but not Rac1 and Cdc42 (Figure S2B). To generate a form of E5 predicted to be inactive as a GEF, we mutated these three conserved amino acids (L562, Q566, and R567) to alanine (E5-LQR). Using the GST-RBD pull-down assay we found that although E5-WT and E5-LQR are expressed at similar levels, the E5-LQR mutant is significantly impaired relative to WT in its ability to activate RhoA (Figure 2B). As a control, we mutated other conserved residues within the α5 DH region to alanine (Q547, S548, R555, and L556). When we tested this mutant we observed no defect in RhoA activation, suggesting that the E5-LQR mutation specifically disrupts the GEF activity of E5 and that the inability of the LQR mutant to activate RhoA is not a general consequence of disrupting the α5 region of Ephexin5 (Figure S2C). Taken together, these findings indicate that E5 requires an intact conserved GEF domain to promote RhoA activity in 293 cells, suggesting that E5 functions as a RhoA GEF.

We next asked if E5 expression affects RhoA activity in the brain. We lysed P3 whole brains from wild-type or *E5*$^{-/-}$ mice and performed a GST-RBD pull-down assay. This analysis revealed a significant decrease in RhoA activation in brain extracts from *E5*$^{-/-}$ mice compared to wild-type mice, suggesting that E5 is required to maintain wild-type levels of RhoA activity in the brain (Figure 2C).

Ephexin5 Negatively Regulates Excitatory Synapse Number

Our findings indicate that E5 interacts with EphB, a key regulator of excitatory synapse development. Thus, we asked whether E5 plays a role in the development of excitatory synapses. We generated two short hairpin RNA constructs that each knocks down E5 protein levels when expressed in 293 cells or cultured hippocampal neurons (Figures S3A–S3B). These shRNAs were introduced into cultured hippocampal neurons together with a plasmid that drives expression of green fluorescent protein (GFP) to allow detection of the transfected cells. We found by staining with α-N-E5 antibodies that the E5 shRNAs (E5-shRNA), but not scrambled hairpin control shRNAs (ctrl-shRNA), efficiently knocked down E5 expression in the transfected neurons (Figure S3C).

By staining with antibodies that recognize pre- and postsynaptic proteins or by visualizing dendritic spines in GFP transfected neurons we observed a significant increase in the number of excitatory synapses and dendritic spines that are present on the E5-shRNA-expressing neurons compared to neurons expressing ctrl-shRNAs (Figures 3A and 3B). By contrast, we failed to detect a significant change in dendritic spine length or width under these conditions (Figure S3D). These findings suggest that E5 functions to restrict spine/excitatory synapse number but has no significant effect on spine morphology. Consistent with these conclusions, we found that overexpression of E5 in hippocampal neurons leads to a decrease in the number of excitatory synapses that are present on the E5-overexpressing neurons (Figure 3C). This ability of E5 to negatively regulate

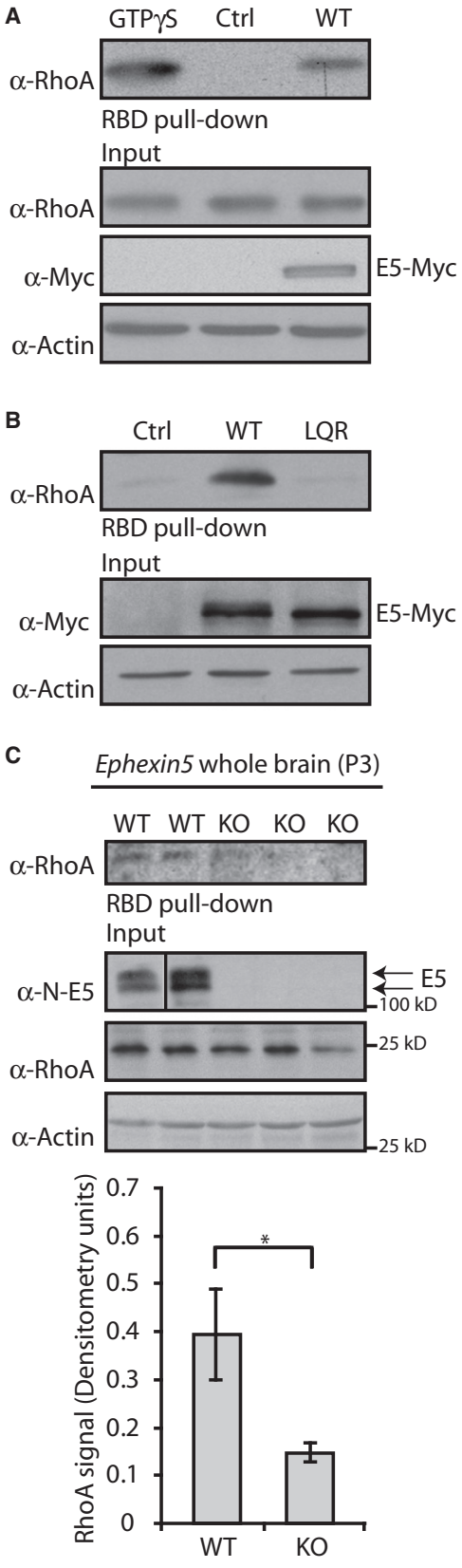

Figure 2. Ephexin5 Is a GEF that Activates RhoA

(A) Lysates from 293 cells transfected with empty vector (Ctrl) or E5-Myc overexpressing vector (WT) were assayed for endogenous RhoA activity using the RBD pull-down assay and analyzed by immunoblotting with an antibody to RhoA (top). GTPγS lane is a positive control for inducing RhoA activity. Increased endogenous RhoA activity is demonstrated by presence of α-RhoA signal in RBD pull-down lanes. Input protein levels and α-Actin loading control are shown (bottom).

(B) Lysates from 293 cells transfected with empty vector (Ctrl), E5-Myc (WT) or LQR mutant of E5-Myc (LQR) were assessed for RhoA activity as measured by RBD assay described in (A). Input protein levels and α-Actin loading control are shown (bottom).

(C) Presence of E5 is critical for wild-type levels of endogenous RhoA signaling in vivo. P3 mouse whole brain lysates from WT or $E5^{-/-}$ (KO) littermates were subjected to RBD pull-down assays as described in (A). A representative immunoblot is shown (top). From three experiments, blinded to condition, the quantification of α-RhoA signal in the RBD pull-down assay was normalized to input RhoA signal (bottom). Error bars indicate ± SEM; *p < 0.05.

See also Figure S2.

excitatory synapse number requires its RhoA GEF activity, as overexpression of E5-LQR had no effect on synapse number (Figure 3D).

To assess the effect of reducing E5 levels on the functional properties of excitatory synapses, we recorded miniature excitatory postsynaptic currents (mEPSCs) from cultured hippocampal neurons transfected with E5-shRNA or ctrl-shRNA. We observed an increase in the frequency and amplitude of mEPSCs on neurons expressing E5-shRNA compared to ctrl-shRNA (Figure 3E). This suggests that E5 acts postsynaptically to restrict excitatory synapse function. The increase in mEPSC frequency could be due to an increase in presynaptic vesicle release onto the transfected neuron or an increase in the number of excitatory synapses that are present on the transfected neuron. We favor the latter possibility since our transfection protocol selectively reduces E5 levels postsynaptically and also because an increase in synapse number would be most consistent with the increase in costaining of pre- and postsynaptic markers that we observe when the level of E5 is reduced. The possibility that E5 functions postsynaptically is further supported by immunofluorescence staining experiments demonstrating that E5 is enriched in dendrites relative to axons (Figure S1F).

As an independent means of assessing the importance of E5 in the control of excitatory synapse number, we cultured hippocampal neurons from *E5*$^{-/-}$ mice or their wild-type littermates for 10 days in vitro and then, following transfection of a GFP-expressing plasmid into these neurons, quantified the number of excitatory synapses present on the transfected neuron at DIV14. We observed a three-fold increase in the number of synapses that are present on *E5*$^{-/-}$ neurons compared to *E5*$^{+/-}$ neurons (Figure 4A). Taken together with the E5-shRNA knockdown and E5 overexpression analyses, these findings suggest that E5 acts postsynaptically to reduce excitatory synapse number.

We next asked if E5 regulates synapse number in the context of an intact developing neuronal circuit using conditional E5 (*E5*$^{fl/fl}$) animals (see Figure S1). Upon introduction of Cre recombinase into *E5*$^{fl/fl}$ cells, exons 4–8 of the *E5* gene are excised resulting in a cell that no longer produces E5 protein (data not

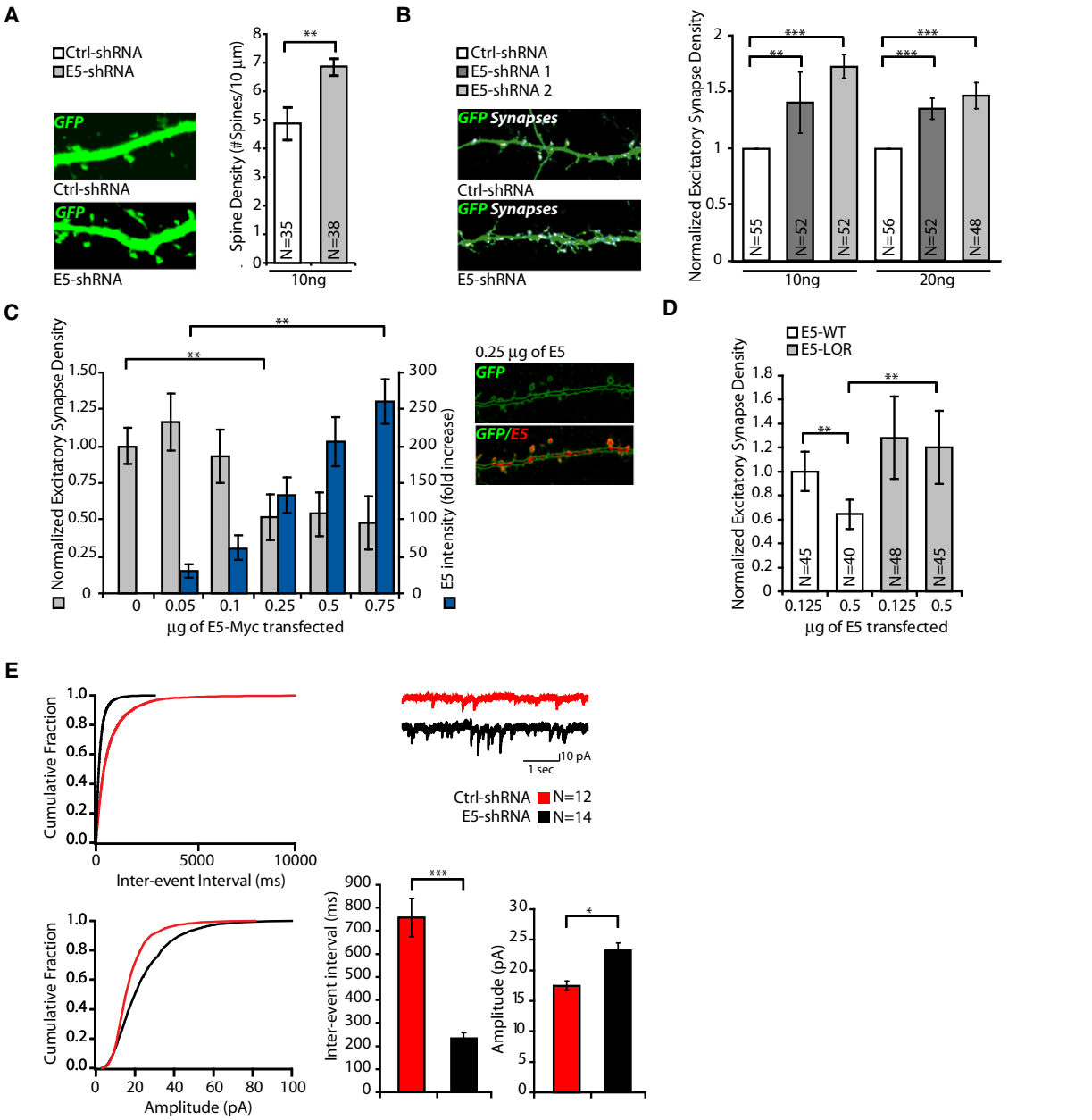

Figure 3. Ephexin5 Negatively Regulates Excitatory Synapse Number

(A) 10 ng of E5-shRNA or Ctrl-shRNA was cotransfected with GFP into rat hippocampal neurons at DIV14. At DIV18 dendritic spines were measured as described in methods. Representative image illustrates dendritic spines. N indicates number of neurons assessed. Error bars indicate ± SEM; **p < 0.01, ANOVA.

(B) 10 ng or 20 ng of two different E5-shRNA or Ctrl-shRNA constructs were cotransfected with GFP into rat hippocampal neurons at DIV10. At DIV14 excitatory synapses were measured as described in methods. Representative image illustrates quantified synapse puncta (white). Error bars indicate ± SEM; **p < 0.01, ***p < 0.005, ANOVA.

(C) DIV10 rat hippocampal neurons were cotransfected with GFP and increasing concentrations of E5-Myc or control plasmid. At DIV 14 excitatory synapses (gray bars) and exogenous E5 expression (blue bars) were measured as described in methods. Representative image illustrates localization of E5-Myc on transfected neuron (red). Error bars indicate ± SEM; **p < 0.01, ANOVA.

(D) Neurons were transfected with E5-Myc (E5-WT) or E5-LQR-Myc (E5-LQR) and quantified as in (C). Error bars indicate ± SEM; **p < 0.01, ANOVA.

(E) Quantification of mEPSC inter-event interval and amplitude from hippocampal neurons transfected as in (B) with 20 ng of shRNA. Cumulative distribution plots, bar graphs and representative traces are shown. Error bars represent the standard deviation of the mean, ***p < 0.005, *p < 0.05.

See also Figure S3 and Figure S1.

shown). Organotypic slices were prepared from the hippocampus of the $E5^{fl/fl}$ mice or their wild-type littermates. Using the biolistic transfection method, a plasmid expressing Cre recombinase was introduced into a low percentage of neurons in the slices. We found that introduction of a Cre-expressing plasmid into $E5^{fl/fl}$ neurons in the hippocampal slice led to a significant increase in the density of dendritic spines present on the Cre-expressing neurons relative to wild-type hippocampal slices transfected with Cre (Figure 4B). The length and width of dendritic spines analyzed in these experiments showed no significant difference between wild-type and $E5^{-/-}$ neurons (Figure S4). Thus, elimination of E5 expression in neurons in the context of an intact neuronal circuit leads to an increase in the number of dendritic spines.

To assess the role of E5 in hippocampal circuit development in vivo, we performed acute slice physiology experiments in the CA1 region of the hippocampus from wild-type or $E5^{-/-}$ mice. We find that relative to wild-type neurons, in $E5^{-/-}$ CA1 pyramidal neurons there are more frequent excitatory events that have larger amplitude (Figure 4C). A possible explanation for these findings is that when E5 function is disrupted during in vivo development more excitatory synapses form resulting in more excitatory postsynaptic events. To test this possibility, we used array tomography to quantify the number of excitatory synapses that form in the CA1 stratum radiatum of wild-type and $E5^{-/-}$ mice. We observed a ~2-fold increase in the number of excitatory synapses within the CA1 region of the $E5^{-/-}$ hippocampus compared to wild-type mice (Figure 4D). Specifically, the number of juxtaposed synapsin and PSD-95 puncta was quantified and considered a measurement of the number of excitatory synapses that form within the CA1 region of the hippocampus in vivo. This analysis revealed a significant increase in the number of PSD-95 puncta but no change in the number of synapsin puncta density (Figure 4D). This suggests that the increase in excitatory synapse number in the stratum radiatum of $E5^{-/-}$ mice is likely due to the absence of E5 postsynaptically and that when E5 is present within dendrites it functions to negatively regulate synapse number in vivo. On the basis of these results, we conclude that a key function of E5 is to restrict excitatory synapse number during the development of neuronal circuits.

Ephexin5 Restricts EphB2 Control of Excitatory Synapse Formation

We next considered the possibility that the ability of E5 to restrict excitatory synapse number might be controlled by EphB2 signaling. To test this idea, we asked whether reducing EphB2 signaling eliminates the increase in excitatory synapse number detected when E5 levels are knocked down by expression of E5-shRNA. To block EphB2 activation, we introduced into neurons a kinase dead version of EphB2 (EphB2-KD) which has been previously shown to block EphB2 signaling (Dalva et al., 2000). As described above, expression of E5-shRNA in neurons leads to a significant increase in the number of synapses that are present on the E5-shRNA-expressing neuron. However, this increase was reversed if the E5-shRNA was cotransfected with a plasmid that drives expression of EphB2-KD, but was not affected by cotransfection of a control plasmid (Figure 4E). These findings suggest that the increase in excitatory synapse number that occurs when E5 levels are reduced requires EphB signaling. Consistent with this conclusion, we find that if we overexpress wild-type EphB2 in neurons more synapses are present on the EphB-expressing neuron. However, this effect is reduced if E5 is overexpressed in neurons together with EphB (Figure 4F). It is possible that the ability of overexpressed E5 to suppress the synapse-promoting effect of EphB2 reflects independent actions of these two signaling molecules. However, given that EphB2 and E5 interact with one another in neurons, the most likely interpretation of these results is that E5 functions directly to restrict the synapse-promoting effects of EphB2. If this were the case, we would predict that for EphB2 to positively regulate excitatory synapse development it would be necessary to inactivate and/or degrade E5.

EphB Mediates Phosphorylation of Ephexin5 at Tyrosine-361

We considered the possibility that since EphB2 is a tyrosine kinase it might inhibit the GEF activity or expression of the E5 protein by catalyzing the tyrosine phosphorylation of E5. In support of this possibility, stimulation of dissociated mouse hippocampal neurons with EphrinB1 (EB1) for 15 min led to an increase in the level of E5 tyrosine phosphorylation as detected by probing immunoprecipitated E5 with the pan-anti-phosphotyrosine antibody, 4G10 (Figure 5A).

We have previously shown that EphrinA1 stimulation of cultured neurons leads to the tyrosine phosphorylation of E1 at tyrosine 87 (Sahin et al., 2005). On the basis of this finding we hypothesized that exposure of neurons to EB1 might promote the phosphorylation of the analogous tyrosine residue (Y361) on E5 (Figure 5B) and that phosphorylation at this site might lead to E5 inactivation. To address this possibility, we overexpressed EphB2 in 293 cells together with wild-type E5 or a mutant form of E5 in which Y361 is converted to a phenylalanine (E5-Y361F). Lysates were prepared from the transfected cells and after SDS-PAGE were immunoblotted with 4G10 (Figure 5C). We found that in the presence of EphB2, E5-WT, but not E5-Y361F, becomes tyrosine phosphorylated. These findings suggest that EphB2 catalyzes the tyrosine phosphorylation of E5 primarily at Y361.

To show definitively that E5 Y361 is tyrosine phosphorylated, we generated an E5 phospho-Y361 antibody (α-pY361). To demonstrate that this antibody specifically recognizes the Y361-phosphorylated form of E5, we immunoblotted cell lysates prepared from 293 cells that express EphB2 and either E5-WT or E5-Y361F with α-pY361. This analysis demonstrated that α-pY361 bind to wild-type E5 but not E5-Y361F (Figure 5C). Furthermore, using α-pY361 we found that when wild-type EphB2, but not a kinase dead or cytoplasmic truncated version of EphB2, is expressed in 293 cells together with E5, E5 becomes phosphorylated at Y361 (Figure S5A). In contrast, when EphA4 or EphA2 were expressed in 293 cells we detected little to no phosphorylation of E5 at Y361 (Figure S5B). These findings suggest that EphB2, but not EphAs, promote E5 Y361 phosphorylation (pY361).

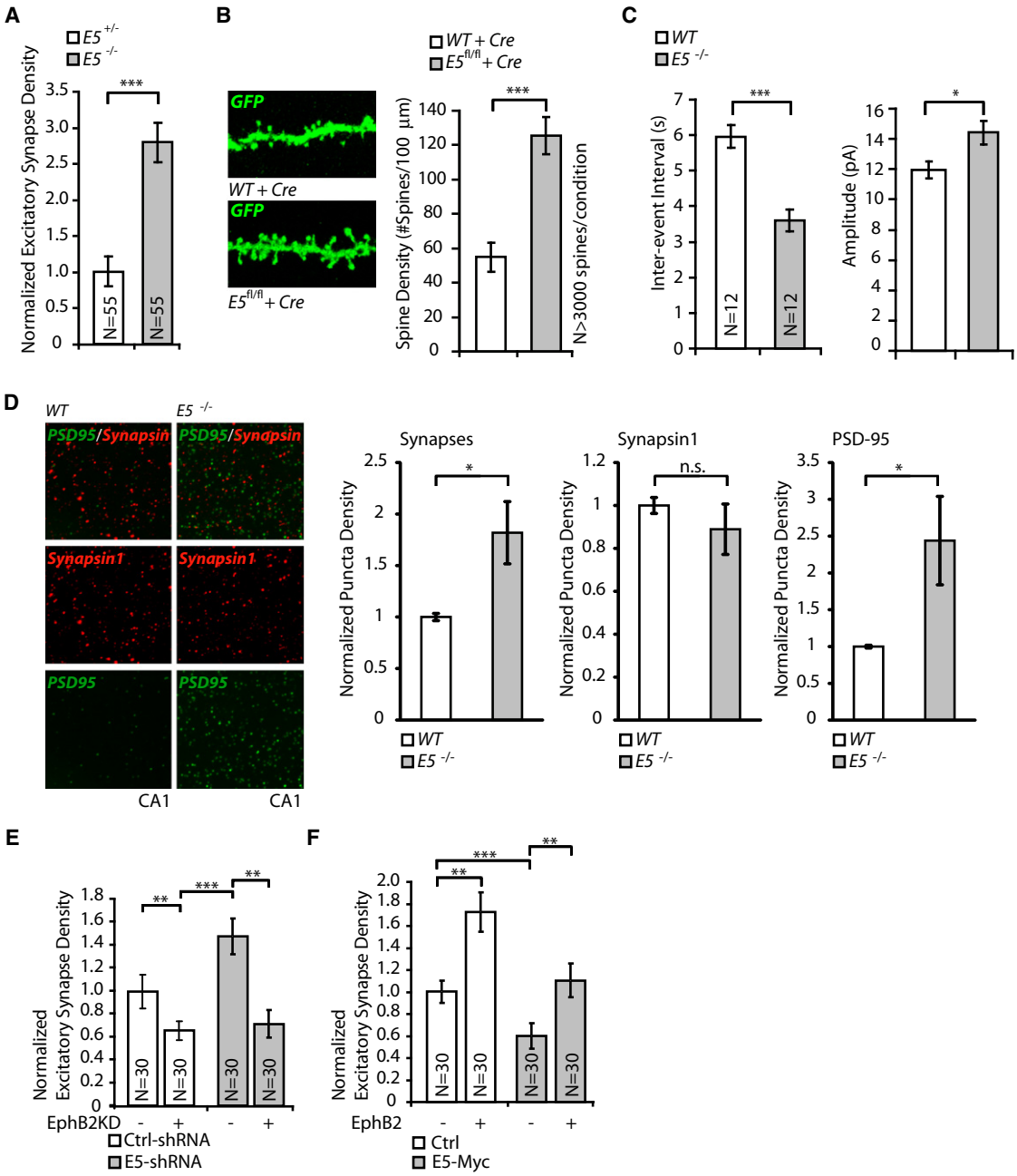

Figure 4. Ephexin5 Restricts EphB2 Control of Excitatory Synapse Formation

(A) E16 hippocampi from $E5^{+/-}$ or $E5^{-/-}$ mice were dissected and dissociated for culture. At DIV10 dissociated neurons were transfected with GFP. At DIV14 neurons were fixed, stained, and excitatory synapses were measured as described in methods. Error bars indicate ± SEM; ***p < 0.005, ANOVA.

(B) Organotypic slices from WT or $E5^{fl/fl}$ mice were biolistically transfected with Cre-recombinase (Cre) and dendritic spines were quantified as described in methods. Representative images are shown (left). Error bars indicate ± SEM; ***p < 0.005, KS test.

(C) Quantification of mEPSC inter-event interval and amplitude from acute hippocampal brain slices prepared from P12-P14 WT or $E5^{-/-}$ mice. Error bars represent the standard deviation of the mean; ***p < 0.005, *p < 0.05.

(D) Hippocampi from three independent littermate pairs consisting of P12 WT and $E5^{-/-}$ mice were prepared as described in methods for quantification of synapses, Synapsin1 and PSD-95 using array tomography. Error bars ± SEM; *p < 0.05, Mann-Whitney U-Test.

(E) Increase in excitatory synapse number following loss of E5 requires EphB2 signaling. At DIV10, control plasmid (–) or EphB2KD plasmid (+) were coexpressed in dissociated mouse hippocampal neurons with GFP and either Ctrl-shRNA or E5-shRNA. At DIV14 excitatory synapses were measured as described in methods. Error bars indicate ± SEM; **p < 0.01, ***p < 0.005, ANOVA.

We also found by immunoblotting with α-pY361 that E5 is phosphorylated at Y361 in the hippocampus of wild-type but not *E5*$^{-/-}$ mice (Figure S5C), and that EB1 stimulation of cultured hippocampal neurons leads to E5 Y361 phosphorylation (Figure 5D). By immunofluorescence microscopy we detect punctate α-pY361 staining along the dendrites of EB1-treated wild-type neurons, but less staining in untreated neurons (Figure 5E). This result suggests that E5 becomes newly phosphorylated at Y361 upon exposure of hippocampal neurons to EB1.

EphB2-Mediated Degradation of Ephexin5 Is Kinase- and Proteasome Dependent

We asked if EB1 stimulation of E5 Y361 phosphorylation leads to a change in E5 activity or expression. To investigate this possibility we asked if EphB suppresses E5-dependent RhoA activation in a phosphorylation-dependent manner. We transfected 293 cells with E5 in the presence or absence of EphB2 and measured RhoA activity using the RBD pull-down assay (Figure 5F). We found that E5-dependent RhoA activation was reduced in 293 cells expressing EphB2 and E5 compared to cells expressing E5 alone. These findings are consistent with the possibility that EphB2-mediated tyrosine phosphorylation of E5 either leads to a suppression of E5's ability to activate RhoA, or alternatively might trigger a decrease in E5 protein expression resulting in a decrease in RhoA activation. We found this latter possibility to be the case (Figure 5F, E5 loading control). Furthermore, when we compared lysates from the brains of wild-type or *EphB2*$^{-/-}$ mice, we observed that E5 phosphorylation at Y361 is decreased while the levels of E5 expression are increased in the lysates from *EphB2*$^{-/-}$ mice (Figure 5G). These data suggest that EphB2 functions to phosphorylate and degrade E5.

Consistent with the idea that E5 expression is destabilized in the presence of EphB, we observed that in the dendrites of cultured hippocampal neurons overexpressing EphB2, endogenous E5 expression levels are reduced compared to control transfected neurons or neurons transfected with a kinase dead version of EphB2 (Figures S6A and S6B). When neurons were exposed to EB1 compared to EA1 for 60 min, we found by immunoblotting of neuronal extracts, or immunofluorescence staining with α-N-E5, that exposure to EB1 leads to a decrease in E5 expression (Figure 6A). The lack of complete loss of E5 expression by Western blot may be due to the fact that EB1 stimulation leads to dendritic and not somatic loss of E5 expression. Moreover, immunofluorescence staining revealed a loss of E5 puncta specifically within the dendrites of EB1-stimulated neurons, consistent with the possibility that EB1/EphB-mediated degradation of E5 relieves an inhibitory constraint that suppresses excitatory synapse formation on dendrites (Figure 6A). In support of this idea, we find by immunoblotting of extracts from mouse hippocampi that endogenous E5 protein levels are highest at postnatal day 3 prior to the time of maximal synapse formation and then decrease as synapse formation peaks in the postnatal period (Figure S6C). Northern blotting revealed that this decrease in E5 protein is not due to a change in the level of E5 mRNA expression (Figure S6C). Given that E5 protein levels decrease dramatically during the time period P7-P21 when synapse formation is maximal, these findings suggest that E5 may need to be degraded prior to synapse formation.

We asked whether EphB-mediated degradation of E5 could be reconstituted in heterologous cells. When EphB and Myc-tagged E5 were coexpressed in 293 cells we observed a significant decrease in E5 protein expression in the presence of EphB2 (Figure 6B). The presence of EphB2 had no effect on the level of expression of a related GEF, E1 (Figure 6B). We asked whether EphB-mediated degradation of E5 depends upon Y361 phosphorylation. We found that in 293 cells overexpressing Myc-tagged E5, the coexpression of EphB2, but not EphB2-KD, resulted in a significant decrease in E5 levels (Figure 6C). This suggests that EphB tyrosine kinase activity is required for E5 degradation. The EphB-mediated reduction in E5 levels is dependent on Y361 phosphorylation, as EphB2 expression had no effect on the level of E5 Y361F expression (Figure 6D). This suggests that the phosphorylation of E5 at Y361 triggers E5 degradation.

We considered the possibility that the Y361 phosphorylation-dependent decrease in E5 protein levels might be due to EphB-dependent stimulation of E5 proteasomal degradation. Consistent with this possibility we found that addition of the proteasome inhibitor lactacystin to 293 cells leads to a reversal of the EphB-dependent decrease in E5 protein levels, as measured by an increase in total ubiquitinated E5 (Figure S6D). In addition, in neuronal cultures the EB1 induced decrease in E5 protein expression is blocked if the proteasome inhibitor lactacystin is added prior to EB1 addition (Figure 6E). Notably, in the presence of lactacystin, E5 is ubiquitinated, further supporting the idea that E5 is degraded by the proteasome.

To test whether E5 is ubiquitinated in the brain, we incubated wild-type or *E5*$^{-/-}$ brain lysates with α-C-E5 and after immunoprecipitation and SDS-PAGE, probed with α-ubiquitin antibodies. This analysis detected the presence of ubiquitinated species in α-C-E5 immunoprecipitates prepared from wild-type but not *E5*$^{-/-}$ brain lysates (Figure 6F). These findings indicate that E5 is ubiquitinated in the brain.

EphB2-Mediated Degradation of Ephexin5 Requires Ube3A

During proteasome-dependent degradation of proteins, specificity is conferred by E3 ligases or E2 conjugating enzymes that recognize the substrate to be degraded. The E3 ligase binds to the substrate and catalyzes the addition of polyubiquitin side chains to the substrate thereby promoting degradation via the proteasome (Hershko and Ciechanover, 1998). We considered several E3 ligases that have recently been implicated in synapse development as candidates that catalyze E5 degradation. One of these E3 ligases, Cbl-b, has previously been implicated in the degradation of EphAs and EphBs (Fasen et al., 2008; Sharfe et al., 2003). A second E3 ligase, Ube3A, has been shown to

(F) E5 can suppress an EphB2-mediated increase in excitatory synapse number. At DIV10, control plasmid (−) or EphB2-expressing plasmid (+) were coexpressed in dissociated mouse hippocampal neurons with GFP and either control (Ctrl) plasmid or E5-Myc plasmid. At DIV14 excitatory synapses were measured as described in methods. Error bars indicate ± SEM; $^{**}p < 0.01$, $^{***}p < 0.005$, ANOVA.
See also Figure S4 and Figure S1.

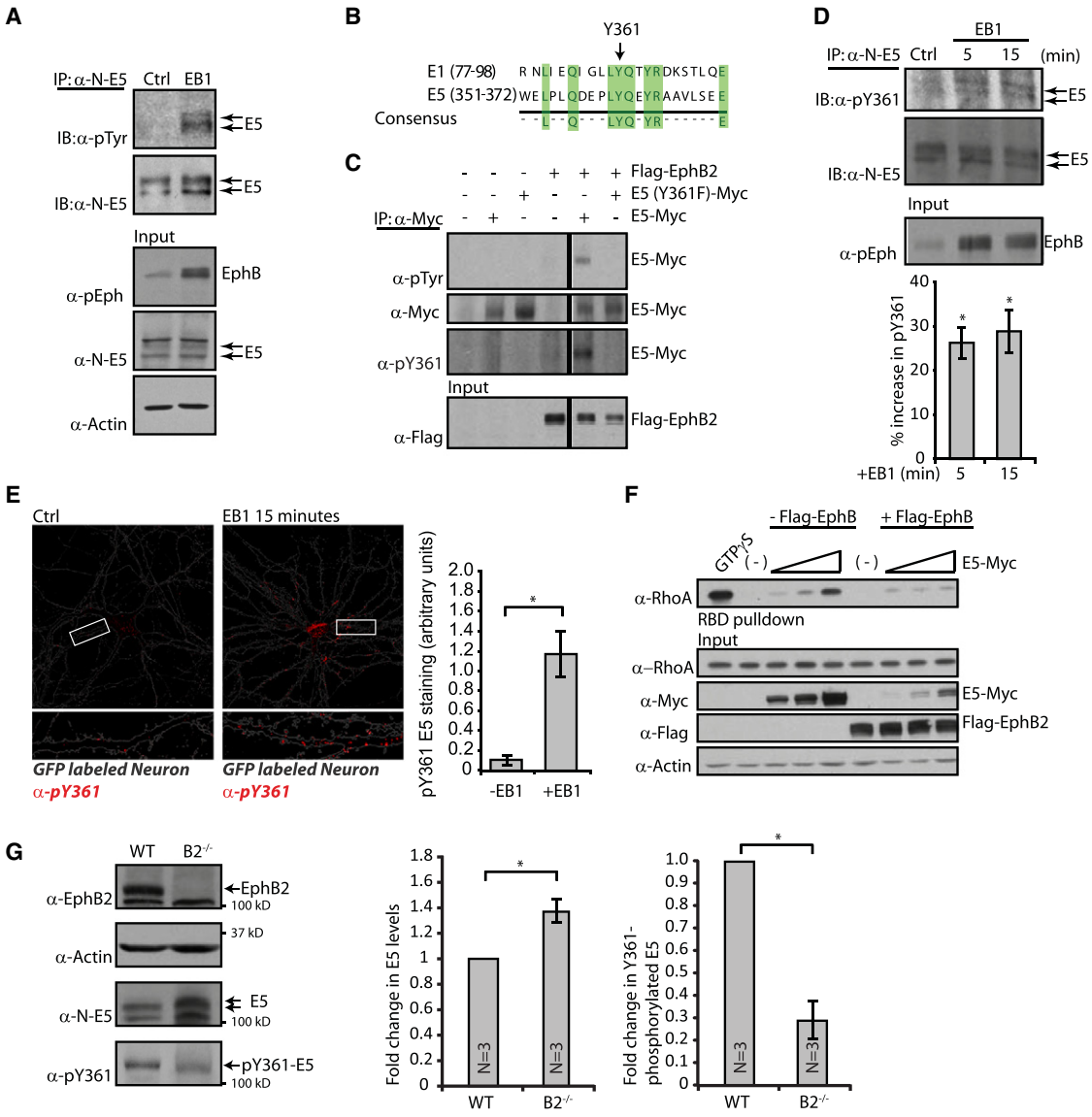

Figure 5. EphB2 Mediates Phosphorylation of Ephexin5 at Tyrosine-361

(A) Dissociated mouse hippocampal neurons were stimulated with either α -Fc IgG (Ctrl) or preclustered Fc-EB1 for 15 min. Neuronal lysates were immunoprecipitated with α-N-E5, followed by immunoblotting for panphosphotyrosine (α-pTyr) or E5 with α-N-E5. EB1 stimulation was determined by immunoblotting neuronal lysates for phospho-Eph (pEph). Input protein levels and α-Actin loading control are shown (bottom).

(B) E5-Y361 is a conserved residue with E1-Y87 (Sahin et al., 2005).

(C) Immunoprecipitation with α-Myc from 293 cell lysates previously transfected with various combinations of overexpressing plasmids containing E5-Myc, E5 (Y361F)-Myc and/or EphB2-Flag, followed by immunoblotting with α-pTyr, α-Myc, α-pY361 or α-Flag. Input EphB2 levels are shown (bottom).

(D) Neurons were treated and lysates prepared as in panel (A) followed by immunoblotting with α-pY361 or α-N-E5. Representative immunoblot with input phospho-Eph (pEph) levels is shown (top). Quantification of three independent experiments is shown as a percent increase in pY361 over Ctrl stimulation (bottom). Error bars indicate ± SEM; *p < 0.05.

(E) Dissociated rat hippocampal neurons were transfected with GFP (gray) and stimulated as in panel (A), followed by fixing and staining for endogenous phosphorylated E5 using α-pY361 (Red). Representative image shown (left). White rectangle outlines magnified dendritic region showing examples of phospho-E5 staining (left bottom). Four independent experiments were imaged and analyzed for pY361 (bar graph). Error bars indicate ± SEM; *p < 0.05.

(F) Lysates from 293 cells transfected with empty vector (-) or increasing concentrations of E5-Myc with or without Flag-EphB2 were assessed for endogenous RhoA activity by RBD assay (previously described). GTPγS lane is a positive control for inducing RhoA. Input protein levels and α-Actin loading control are shown (bottom).

(G) WT and EphB2$^{-/-}$ (B2$^{-/-}$) brain lysates were immunoblotted with α-EphB2, α-N-E5, α-Actin, or α-pY361 according to methods (left). Quantification of α-N-E5 or α-pY361 signal from three independent experiments is normalized to α-Actin and represented as fold change compared to wild-type. Error bars indicate ± SEM; *p < 0.05.

See also Figure S5.

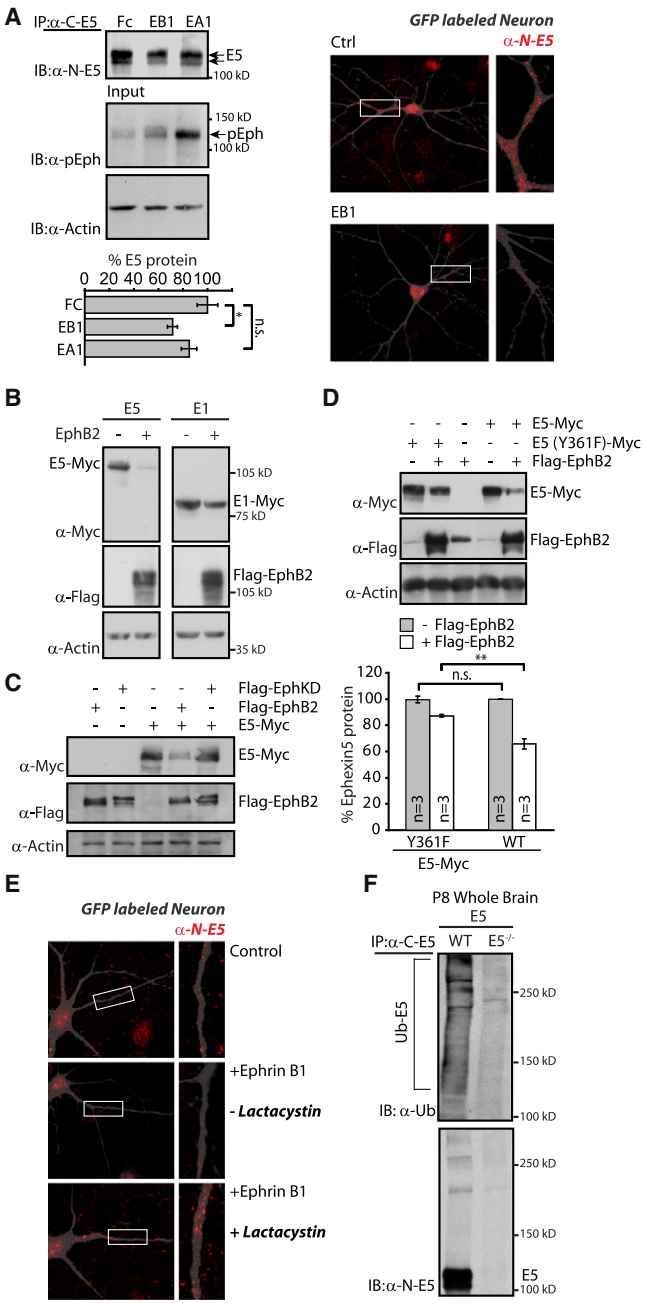

Figure 6. EphB2-Mediated Degradation of Ephexin5 Is Kinase- and Proteasome Dependent

(A) Dissociated mouse hippocampal neurons were incubated with preclustered Fc, Fc-EB1 or Fc-EA1 for 60 min, lysed, and immunoprecipitated with α-C-E5 followed by immunoblotting with α-N-E5. Immunoblot of input with α-pEph or α-Actin (loading control) are shown. Western is one representative image, and quantification is of three separate experiments with samples normalized to α-Actin (left). Error bars indicate ± SEM; *$p < 0.05$. Right, dissociated mouse hippocampal neurons were transfected with GFP (gray) and stimulated with either preclustered Fc (Ctrl) or Fc-EB1 (EB1) for 30 min, followed by fixing and staining for endogenous E5 using α-N-E5 (red). White rectangle outlines magnified dendritic region showing examples of E5 staining (right).

(B) Lysates from 293 cells previously transfected with various combinations of overexpressing plasmids containing E5-Myc, E1-Myc and/or Flag-EphB2 were immunoblotted with α-Myc, α-Flag, or α-Actin (loading control).

(C) Lysates from 293 cells previously transfected with various combinations of overexpressing plasmids containing Flag-EphB2, Flag-EphB2KD and/or E5-Myc were immunoblotted with α-Myc, α-Flag, or α-Actin (loading control).

(D) Lysates from 293 cells previously transfected with various combinations of overexpressing plasmids containing E5-Myc, E5-Y361F-Myc and/or Flag-EphB2 were immunoblotted with α-Myc, α-Flag, or α-Actin (loading control). Representative immunoblot is shown (top). From three independent experiments E5 levels were quantified and normalized to E5 expression in absence of EphB2-Flag (bottom). Error bars indicate ± SEM; **$p < 0.01$.

(E) Dissociated mouse hippocampal neurons transfected with GFP (gray) were stimulated similar to (B) in the absence or presence of lactacystin and immunostained with α-N-E5. White rectangle outlines magnified dendritic region showing examples of E5 staining (right).

(F) WT and $E5^{-/-}$ brains were lysed and immunoprecipitated with α-C-E5 followed by immunoblotting with α-ub or α-N-E5.

See also Figure S6.

regulate synapse number. To determine if Ube3A and/or Cbl-b catalyze E5 degradation we first asked if either of these E3 ligases interacts with and degrades E5 in 293 cells. When these E3 ligases were epitope-tagged and expressed in 293 cells together with E5 we found that E5 coimmunoprecipitates with Ube3A but not with Cbl-b (Figure 7A). The coimmunoprecipitation of Ube3A with E5 was specific in that Ube3A was not coimmunoprecipitated with two other neuronal proteins, E1 or the transcription factor MEF2. In a previous study we have shown that Ube3A binds to substrates via a Ube3A binding domain (hereafter referred to as UBD [Greer et al., 2010]). Using protein sequence alignment programs, ClustalW and ModBase, we identified a UBD in E5, providing further support for the idea that E5 might be a substrate of Ube3A (Figure S7A). Consistent with this hypothesis, we found that the level of E5 expression is reduced in 293 cells cotransfected with titrating amounts of Ube3A compared to cells cotransfected with titrating amounts of Cbl-b (Figure S7B).

We asked if EB1/EphB-mediated E5 degradation in neurons is catalyzed by Ube3A. To inhibit Ube3A activity we introduced into neurons a dominant interfering form of Ube3A (dnUbe3A) that contains a mutation in the ubiquitin ligase domain rendering Ube3A inactive. We have previously shown that even though dnUbe3A is catalytically inactive it still binds to E2 ligases and to its substrates and functions in a dominant negative manner to block the ability of wild-type Ube3A to ubiquitinate its substrates (Greer et al., 2010). We found that when introduced into 293 cells dnUbe3A binds to E5 (Figure 7A). We also found by immunofluorescence microscopy that when overexpressed in neurons, dnUbe3A blocks EB1/EphB stimulation of E5 degradation (Figure 7B). EB1/EphB stimulation of E5 degradation was also attenuated when Ube3A expression was knocked down by a shRNA that specifically targets the Ube3A mRNA (Figure 7B; Greer et al., 2010). Notably, the presence of the dnUbe3A did not affect E5 expression in neurons in the absence of EphrinB stimulation, suggesting that EphrinB stimulation of E5 Y361 phosphorylation may be required for Ube3A-mediated degradation of E5 (Figure S7C).

To determine if Ube3A-dependent degradation of E5 might be relevant to the etiology of Angelman syndrome we asked if the absence of Ube3A in a mouse model of Angelman syndrome affects the level of E5 expression in the brain. We compared

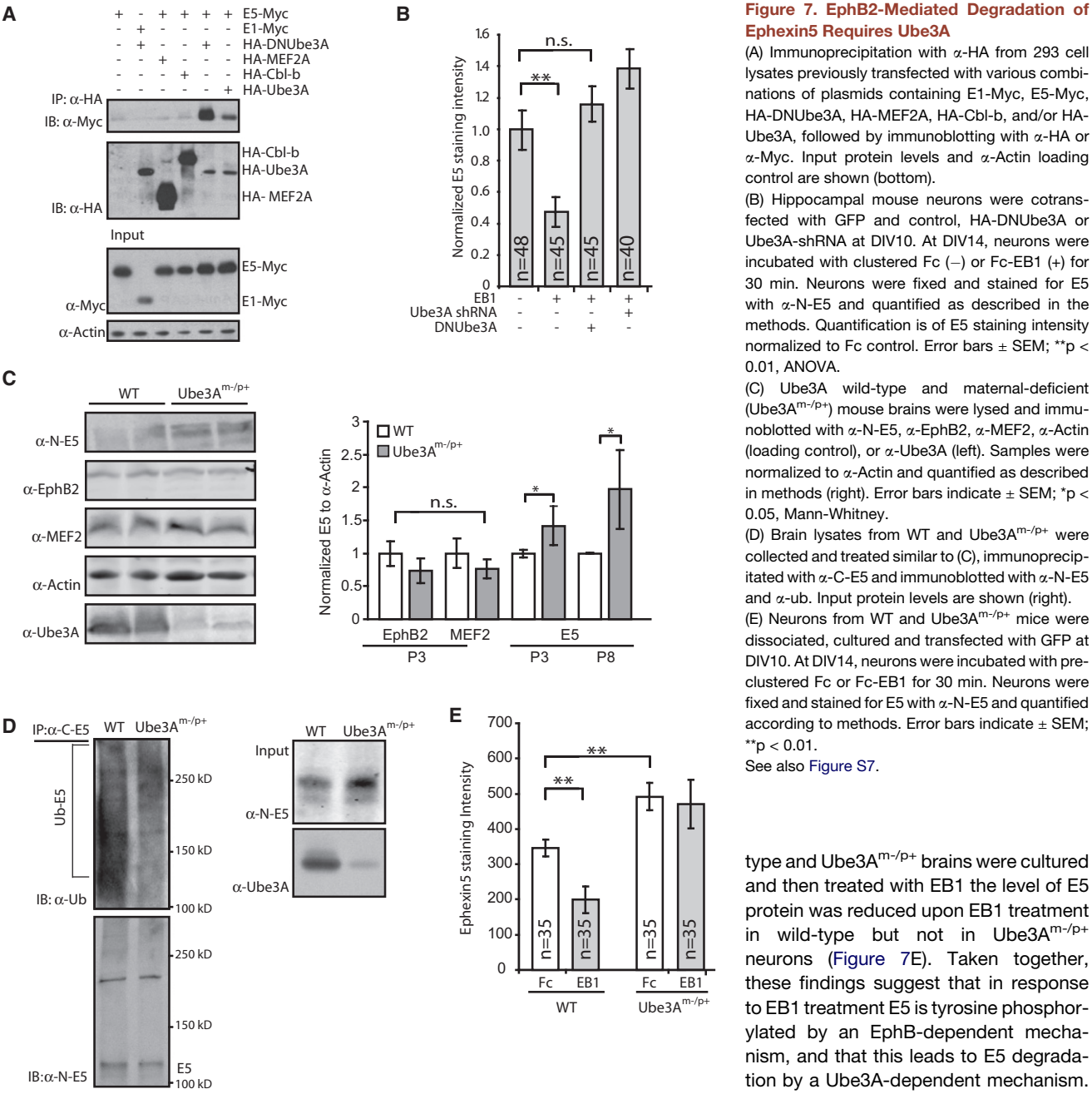

Figure 7. EphB2-Mediated Degradation of Ephexin5 Requires Ube3A

(A) Immunoprecipitation with α-HA from 293 cell lysates previously transfected with various combinations of plasmids containing E1-Myc, E5-Myc, HA-DNUbe3A, HA-MEF2A, HA-Cbl-b, and/or HA-Ube3A, followed by immunoblotting with α-HA or α-Myc. Input protein levels and α-Actin loading control are shown (bottom).

(B) Hippocampal mouse neurons were cotransfected with GFP and control, HA-DNUbe3A or Ube3A-shRNA at DIV10. At DIV14, neurons were incubated with clustered Fc (–) or Fc-EB1 (+) for 30 min. Neurons were fixed and stained for E5 with α-N-E5 and quantified as described in the methods. Quantification is of E5 staining intensity normalized to Fc control. Error bars ± SEM; **p < 0.01, ANOVA.

(C) Ube3A wild-type and maternal-deficient (Ube3A$^{m-/p+}$) mouse brains were lysed and immunoblotted with α-N-E5, α-EphB2, α-MEF2, α-Actin (loading control), or α-Ube3A (left). Samples were normalized to α-Actin and quantified as described in methods (right). Error bars indicate ± SEM; *p < 0.05, Mann-Whitney.

(D) Brain lysates from WT and Ube3A$^{m-/p+}$ were collected and treated similar to (C), immunoprecipitated with α-C-E5 and immunoblotted with α-N-E5 and α-ub. Input protein levels are shown (right).

(E) Neurons from WT and Ube3A$^{m-/p+}$ mice were dissociated, cultured and transfected with GFP at DIV10. At DIV14, neurons were incubated with preclustered Fc or Fc-EB1 for 30 min. Neurons were fixed and stained for E5 with α-N-E5 and quantified according to methods. Error bars indicate ± SEM; **p < 0.01.

See also Figure S7.

the level of E5 protein expression in the brains of wild-type mice to that expressed in the brains of mice in which the maternally inherited Ube3A was disrupted (Ube3A$^{m-/p+}$). Because the paternally inherited copy of Ube3A is silenced in the brain due to imprinting, the level of Ube3A expression in Ube3A$^{m-/p+}$ neurons is very low. We found that the level of E5 expression in the brains of Ube3A$^{m-/p+}$ mice was significantly higher than that detected in the brains of wild-type mice (Figure 7C). Moreover, the level of ubiquitinated E5 in brains of Ube3A$^{m-/p+}$ mice was significantly reduced compared to the brains of litter mate controls (Figure 7D). In addition we found that when neurons from wild-type and Ube3A$^{m-/p+}$ brains were cultured and then treated with EB1 the level of E5 protein was reduced upon EB1 treatment in wild-type but not in Ube3A$^{m-/p+}$ neurons (Figure 7E). Taken together, these findings suggest that in response to EB1 treatment E5 is tyrosine phosphorylated by an EphB-dependent mechanism, and that this leads to E5 degradation by a Ube3A-dependent mechanism. If E5 degradation is disrupted due to a loss of Ube3A as occurs in Angelman syndrome the result is an increase in E5 expression and a disruption of the proper control of excitatory synapse number during brain development.

DISCUSSION

Previous studies have revealed a role for EphrinB/EphB signaling in the development of excitatory synapses (Klein, 2009). However, the regulatory constraints that temper EphB-dependent synapse development so that excitatory synapses form at the right time and place, and in the correct number were not

known. In this study we identify a RhoA GEF, E5, which functions to restrict EphB-dependent excitatory synapse development. E5 interacts with EphB prior to EphrinB binding, and by activating RhoA serves to inhibit synapse development. The binding of EphrinB to EphB as synapses form triggers the phosphorylation and degradation of E5 by a Ube3A-dependent mechanism. The reduction in E5 expression may allow EphB to promote excitatory synapse development by activating Rac and other proteins at the synapse.

The findings that E5 functions to restrict excitatory synapse number suggests that, even though EphBs promote excitatory synapse development, there are constraints on the activity of EphB so that synapse number is effectively controlled. There are several steps in the process of synapse development where E5 may function to restrict synapse number. One possibility is that E5 functions early in development as a barrier to excitatory synapse formation by activating RhoA and restricting the motility or growth of dendritic filopodia that are the sites of contact by the presynaptic neuron. For example, by inhibiting dendritic filopodia formation or motility, E5 may decrease the number of contacts the filopodia make with the presynaptic neuron, thus resulting in the formation of fewer synapses. An alternative possibility is that E5 functions to restrict synapse number later in development perhaps to counterbalance the positive effects of EphB on Rac that promote dendritic spine development. An additional possibility is that E5 functions after excitatory synapse development as a regulator of synapse elimination.

Our analyses of E5 function are most consistent with the possibility that E5 functions early in the process of synapse development. First, we find that E5 is expressed, active, and bound to EphB prior to synapse formation. Second, the interaction of EphrinB with EphB, a process that is thought to be an early step in excitatory synapse development, triggers the degradation of E5. Third, our preliminary time-lapse imaging studies suggest that E5 is localized to newly formed filopodia prior to synapse development where it appears to restrict filopodia motility and growth (Margolis et al. unpublished). Thus, E5 might function as an initial barrier to synapse formation until it is degraded upon EphrinB binding to EphB.

It is possible that through its interaction with EphB, E5 marks the sites where synapses will form, and that the degradation of E5 is a critical early step in excitatory synapse development. While the mechanisms by which E5 is degraded are not fully understood, our studies suggest that the phosphorylation of the N-terminus of E5 at Y361 triggers the Ube3A-mediated proteasomal degradation of E5. One possibility is that prior to pY361 the N- and C-terminal portions of E5 interact, thereby protecting E5 from degradation. The phosphorylation of E5 at Y361 may relieve this inhibitory constraint allowing for E5 ubiquitination and degradation. A similar mechanism has been shown to regulate the activation of the Rac GEF Vav, (Aghazadeh et al., 2000)). During EphrinA/EphA signaling it has been proposed that Vav-mediated endocytosis of the EphrinA/EphA complex may allow the conversion of the initial adhesive interaction between EphrinA and EphA-expressing cells into a repulsive interaction that results in growth cone collapse and axon repulsion. It is possible that E5 has a related function during EphB signaling at synapses. Typically the EB/EphB interaction is thought to be repulsive. This has been documented in studies of EphB's role in the process of axon guidance (Egea and Klein, 2007; Flanagan and Vanderhaeghen, 1998). However, during synapse development the EphrinB/EphB interaction is thought to result in synapse formation, a process that requires an interaction between the developing pre- and postsynaptic specialization. One possibility is that when EphrinB and EphB mediate the interaction between the incoming axon and the developing dendrite, the interaction is facilitated by the degradation of E5 by Ube3A. Since E5 is a RhoA GEF, its presence might initially lead to repulsion between the incoming axon and the dendrite. However, the EphB-dependent degradation of E5 might convert this initial repulsive interaction into an attractive one.

The finding that Ube3A is the ubiquitin ligase that controls EphB-mediated E5 degradation is of interest given the role of Ube3A in human cognitive disorders such as Angelman syndrome and autism. The absence of Ube3A function in Angelman syndrome would be predicted to result in an increase in E5 protein expression, and thus a decrease in EphB-dependent synapse formation. Consistent with this possibility, we find in a mouse model for Angelman syndrome that the level of E5 protein expression is elevated and that in response to EphrinB treatment E5 is not degraded. Likewise, several studies have indicated that synapse development and function is disrupted in these mice (Jiang et al., 1998; Yashiro et al., 2009).

The recent finding that the Ube3A gene lies within a region of chromosome 15 that is sometimes duplicated in autism raises the possibility that altered levels of Ephexin5 and the resulting defects in excitatory synapse restriction might also be a mechanism relevant to the etiology of autism. If this is the case, a possible therapy for treating autism might be to reduce the level of Ube3A activity, and thus increase the level of Ephexin5 expression. It is important to consider that in addition to Ephexin5, Ube3A regulates the abundance of other synaptic proteins. Nevertheless, the ultimate effect of the aberrant expression of Ephexin5 and other Ube3A substrates on synapse development and function will require further study. It seems likely that such studies will provide further understanding of the development of human cognitive function and new insights into how this process goes awry in disorders such as Angelman syndrome and autism.

EXPERIMENTAL PROCEDURES

DNA Constructs

Details of DNA constructs can be found in Supplemental Information.

Generation of E5−/− Mice

An E5 targeting vector was electroporated into 129 J1 ES cells, and positive clones were identified by Southern hybridization with two separate probes (see Supplemental Information).

Antibodies

Details of antibodies can be found in Supplemental Information.

Mice, Cell Culture, Transfections, and Ephrin Stimulations

Ube3A$^{m-/p+}$ mice were previously described (Greer et al., 2010). EphB2 knockout mice were previously described (Kayser et al., 2008). 293T cells were cultured in DMEM + 10% FBS and transfected using the calcium phosphate method. Organotypic slice cultures were prepared from P6 mouse brains

and biolistically transfected. Acute slices were prepared from P12-14 mice. Dissociated neurons were cultured in Neurobasal Medium supplemented with B27 and transfected using the Lipofectamine method. For details on cell culture, transfections, and Ephrin stimulations, see Supplemental Information.

Cell Lysis, Immunoprecipitations, GEF Pull-Down Assays, and Western Blots

Whole rat or mouse brains or cultured cells were collected and homogenized in RIPA buffer. For immunoprecipitations, lysed cells were centrifuged and supernatants were incubated with appropriate antibody for 2 hr at 4°C, followed by addition of Protein-A or Protein-G beads (Santa Cruz Biotechnology) for 1 hr, and washed three times with ice-cold RIPA buffer. For the α-PY361 detection experiment in 293T cells, samples were boiled in SDS buffer to disrupt the E5/EphB2 interaction and diluted 1:5 in 1.25× RIPA buffer prior to immunoprecipitation of E5-Myc. RBD and PBD pull-down assays were conducted according to the manufacture's suggestions (Upstate Cell Signaling Solutions). For details see Supplemental Information.

In Situ Hybridization

To generate probes for in situ hybridization, mouse E5 and EphB2 cDNA were subcloned into pBluescript II SK (+). Bluescript plasmids containing E5 or EphB2 cDNA were linearized using the restriction enzyme BssHII. Sense and antisense probes were generated using DIG RNA labeling mix (Roche) according to manufacturer's instructions. Full-length DIG-labeled probes were subjected to alkaline hydrolysis as described in Supplemental Information.

Immunocytochemistry

Neurons were paraformaldehyde fixed in PBS. For measuring synapse density, fixed neurons were incubated with α-PSD-95 and α-Synapsin antibodies followed by α-Cy3 and α-Cy5 antibodies to visualize the primary antibodies. For protein colocalization experiments fixed neurons were similarly treated using α-EphB2 antibodies and α-N-E5 antibodies or α-pY361-E5. For overexpression studies fixed neurons were incubated using α-Myc or α-Flag antibodies to visualize overexpressed E5-Myc or EphB2-Flag protein in the context of the GFP-labeled neurons. For details see Supplemental Information.

Synapse Assay, Image Analysis, and Quantification

Images were acquired on a Zeiss LSM5 Pascal confocal microscope and spine and synapse analysis was performed as previously described (see Supplemental Information).

Ube3A$^{m-/p+}$ Cultures

Dissociated hippocampal neurons from *Ube3A*$^{m-/p+}$ and wild-type mice were prepared as previously described (Greer et al., 2010).

Array Tomography

Array tomography was performed as previously described (Micheva and Smith, 2007) with modifications as described in the Supplemental Information.

Electrophysiology

Electrophysiology was performed using standard methods (see Supplemental Information).

SUPPLEMENTAL INFORMATION

Supplemental Information includes Extended Experimental Procedures and seven figures and can be found with this article online at doi:10.1016/j.cell.2010.09.038.

ACKNOWLEDGMENTS

We thank M. Thompson, Y. Zhou, and H. Ye for assistance in generating mice; E. Griffith, J. Zieg, S. Cohen, I. Spiegel, M. Andzelm, and the Greenberg lab for critical discussions. This work was supported by National Institute of Neurological Disorders and Stroke grant RO1 5R01NS045500 (M.E.G); NRSA Training grant 5T32AG00222-15 (S.S.M.); and Edward R. and Anne G. Lefler postdoctoral fellowship (S.S.M.).

Received: November 25, 2009
Revised: July 19, 2010
Accepted: September 23, 2010
Published: October 28, 2010

REFERENCES

Aghazadeh, B., Lowry, W.E., Huang, X.Y., and Rosen, M.K. (2000). Structural basis for relief of autoinhibition of the Dbl homology domain of proto-oncogene Vav by tyrosine phosphorylation. Cell *102*, 625–633.

Dalva, M.B., Takasu, M.A., Lin, M.Z., Shamah, S.M., Hu, L., Gale, N.W., and Greenberg, M.E. (2000). EphB receptors interact with NMDA receptors and regulate excitatory synapse formation. Cell *103*, 945–956.

Dalva, M.B., McClelland, A.C., and Kayser, M.S. (2007). Cell adhesion molecules: signalling functions at the synapse. Nat. Rev. Neurosci. *8*, 206–220.

Egea, J., and Klein, R. (2007). Bidirectional Eph-ephrin signaling during axon guidance. Trends Cell Biol. *17*, 230–238.

Ethell, I.M., Irie, F., Kalo, M.S., Couchman, J.R., Pasquale, E.B., and Yamaguchi, Y. (2001). EphB/syndecan-2 signaling in dendritic spine morphogenesis. Neuron *31*, 1001–1013.

Fasen, K., Cerretti, D.P., and Huynh-Do, U. (2008). Ligand binding induces Cbl-dependent EphB1 receptor degradation through the lysosomal pathway. Traffic *9*, 251–266.

Flanagan, J.G., and Vanderhaeghen, P. (1998). The ephrins and Eph receptors in neural development. Annu. Rev. Neurosci. *21*, 309–345.

Fu, W.Y., Chen, Y., Sahin, M., Zhao, X.S., Shi, L., Bikoff, J.B., Lai, K.O., Yung, W.H., Fu, A.K., Greenberg, M.E., et al. (2007). Cdk5 regulates EphA4-mediated dendritic spine retraction through an E1-dependent mechanism. Nat. Neurosci. *10*, 67–76.

Greer, P.L., Hanayama, R., Bloodgood, B.L., Mardinly, A.R., Lipton, D.M., Flavell, S.W., Kim, T.K., Griffith, E.C., Waldon, Z., Maehr, R., et al. (2010). The Angelman Syndrome protein Ube3A regulates synapse development by ubiquitinating arc. Cell *140*, 704–716.

Grunwald, I.C., Korte, M., Wolfer, D., Wilkinson, G.A., Unsicker, K., Lipp, H.P., Bonhoeffer, T., and Klein, R. (2001). Kinase-independent requirement of EphB2 receptors in hippocampal synaptic plasticity. Neuron *32*, 1027–1040.

Grunwald, I.C., Korte, M., Adelmann, G., Plueck, A., Kullander, K., Adams, R.H., Frotscher, M., Bonhoeffer, T., and Klein, R. (2004). Hippocampal plasticity requires postsynaptic ephrinBs. Nat. Neurosci. *7*, 33–40.

Henkemeyer, M., Itkis, O.S., Ngo, M., Hickmott, P.W., and Ethell, I.M. (2003). Multiple EphB receptor tyrosine kinases shape dendritic spines in the hippocampus. J. Cell Biol. *163*, 1313–1326.

Hershko, A., and Ciechanover, A. (1998). The ubiquitin system. Annu. Rev. Biochem. *67*, 425–479.

Jiang, Y.H., Armstrong, D., Albrecht, U., Atkins, C.M., Noebels, J.L., Eichele, G., Sweatt, J.D., and Beaudet, A.L. (1998). Mutation of the Angelman ubiquitin ligase in mice causes increased cytoplasmic p53 and deficits of contextual learning and long-term potentiation. Neuron *21*, 799–811.

Jontes, J.D., Buchanan, J., and Smith, S.J. (2000). Growth cone and dendrite dynamics in zebrafish embryos: early events in synaptogenesis imaged in vivo. Nat. Neurosci. *3*, 231–237.

Kayser, M.S., McClelland, A.C., Hughes, E.G., and Dalva, M.B. (2006). Intracellular and trans-synaptic regulation of glutamatergic synaptogenesis by EphB receptors. J. Neurosci. *26*, 12152–12164.

Kayser, M.S., Nolt, M.J., and Dalva, M.B. (2008). EphB receptors couple dendritic filopodia motility to synapse formation. Neuron *59*, 56–69.

Kishino, T., Lalande, M., and Wagstaff, J. (1997). UBE3A/E6-AP mutations cause Angelman syndrome. Nat. Genet. *15*, 70–73.

Klein, R. (2009). Bidirectional modulation of synaptic functions by Eph/ephrin signaling. Nat. Neurosci. *12*, 15–20.

Lai, K.O., and Ip, N.Y. (2009). Synapse development and plasticity: roles of ephrin/Eph receptor signaling. Curr. Opin. Neurobiol. *19*, 275–283.

Lim, B.K., Matsuda, N., and Poo, M.M. (2008). Ephrin-B reverse signaling promotes structural and functional synaptic maturation in vivo. Nat. Neurosci. *11*, 160–169.

Micheva, K.D., and Smith, S.J. (2007). Array tomography: a new tool for imaging the molecular architecture and ultrastructure of neural circuits. Neuron *55*, 25–36.

Murai, K.K., Nguyen, L.N., Irie, F., Yamaguchi, Y., and Pasquale, E.B. (2003). Control of hippocampal dendritic spine morphology through ephrin-A3/EphA4 signaling. Nat. Neurosci. *6*, 153–160.

Ogita, H., Kunimoto, S., Kamioka, Y., Sawa, H., Masuda, M., and Mochizuki, N. (2003). EphA4-mediated Rho activation via Vsm-RhoGEF expressed specifically in vascular smooth muscle cells. Circ. Res. *93*, 23–31.

Penzes, P., Beeser, A., Chernoff, J., Schiller, M.R., Eipper, B.A., Mains, R.E., and Huganir, R.L. (2003). Rapid induction of dendritic spine morphogenesis by trans-synaptic ephrinB-EphB receptor activation of the Rho-GEF kalirin. Neuron *37*, 263–274.

Rossman, K.L., Der, C.J., and Sondek, J. (2005). GEF means go: turning on RHO GTPases with guanine nucleotide-exchange factors. Nat. Rev. Mol. Cell Biol. *6*, 167–180.

Sahin, M., Greer, P.L., Lin, M.Z., Poucher, H., Eberhart, J., Schmidt, S., Wright, T.M., Shamah, S.M., O'Connell, S., Cowan, C.W., et al. (2005). Eph-dependent tyrosine phosphorylation of ephexin1 modulates growth cone collapse. Neuron *46*, 191–204.

Shamah, S.M., Lin, M.Z., Goldberg, J.L., Estrach, S., Sahin, M., Hu, L., Bazalakova, M., Neve, R.L., Corfas, G., Debant, A., et al. (2001). EphA receptors regulate growth cone dynamics through the novel guanine nucleotide exchange factor ephexin. Cell *105*, 233–244.

Sharfe, N., Freywald, A., Toro, A., and Roifman, C.M. (2003). Ephrin-A1 induces c-Cbl phosphorylation and EphA receptor down-regulation in T cells. J. Immunol. *170*, 6024–6032.

Snyder, J.T., Worthylake, D.K., Rossman, K.L., Betts, L., Pruitt, W.M., Siderovski, D.P., Der, C.J., and Sondek, J. (2002). Structural basis for the selective activation of Rho GTPases by Dbl exchange factors. Nat. Struct. Biol. *9*, 468–475.

Tashiro, A., Minden, A., and Yuste, R. (2000). Regulation of dendritic spine morphology by the rho family of small GTPases: antagonistic roles of Rac and Rho. Cereb. Cortex *10*, 927–938.

Yashiro, K., Riday, T.T., Condon, K.H., Roberts, A.C., Bernardo, D.R., Prakash, R., Weinberg, R.J., Ehlers, M.D., and Philpot, B.D. (2009). Ube3a is required for experience-dependent maturation of the neocortex. Nat. Neurosci. *12*, 777–783.

Ziv, N.E., and Smith, S.J. (1996). Evidence for a role of dendritic filopodia in synaptogenesis and spine formation. Neuron *17*, 91–102.

EXTENDED EXPERIMENTAL PROCEDURES

DNA Constructs

The full-length mouse E5 was generated by RT-PCR from RNA isolated from mouse E16 cortical neurons at 7 days in vitro and subcloned into EcoRI/XhoI sites of the pEF1-Myc-HisA vector (Invitrogen). E5 GEF and phosphorylation mutants (LQR, QSRL, and Y361F) were generated using the QuickChange site-directed mutagenesis kit (Stratagene). All constructs were verified by DNA sequencing. The following plasmid constructs have been described previously: Flag-EphB2, Flag-EphB2KD, Flag-EphB2 ΔCyto (Dalva et al., 2000), Ephexin1-Myc (Sahin et al., 2005), HA-Ube3A (Greer et al., 2010), HA-Mef2 (Flavell et al., 2006), HA-Cbl-b (Cowan et al., 2005), eGFP (Paradis et al., 2007), Cre-recombinase (Lin et al., 2008).

The pLenti-Lox-E5 RNAi constructs were designed as previously described. Briefly, the following oligonucleotides were annealed with their complimentary sequence and inserted into the BglII site of pLenti-Lox vector: TAGCCGCCTTATGGATACAAA and TCCGAAAGCACTTCCTCAAAT (Figure S2). These regions were not homologous to Ephexin1 or any other known genes as indicated by Blast search.

Generation of Ephexin5−/− Mice

An E5 targeting vector was electroporated into 129 J1 ES cells, and positive clones were identified by Southern hybridization with two separate probes. To obtain constitutive deletion of the *E5* exons, a Cre-recombinase expressing plasmid (pOG231Cre or pMC-CreN) was electroporated into ES cells carrying the homologous recombination. Constitutive knockout and conditional floxed ES cells were identified by replicate plating for G418 sensitivity followed by Southern hybridization and genomic PCR. Positive clones were grown without G418 and expanded for genotyping.

Antibodies

The following rabbit polyclonal antibodies were generated against the indicated amino acids of mouse E5 and then affinity purified: α-N-E5 was raised against a GST-fusion protein containing amino acids 1-418. α-C-E5 was raised against a C-terminal peptide sequence corresponding to amino acids 720-732 (EHERRKHLRQHUK). α-p361 was raised against a peptide sequence corresponding to amino acids 354-368 (PLQDEPLpYQTYRAAV), in which tyrosine residue 361 was phosphorylated (denoted as pY in peptide sequence). The specificity of the E5 antibodies was tested by western blotting using brain lysates from WT and E5 knockout littermates. Rabbit polyclonal α-EphB2 and anti-phospho-Eph (α-pEph) were used as previously described (Dalva et al., 2000). The following antibodies are commercially available and used according to manufacturer's suggestions for Western blotting, immunocytochemistry and immunoprecipitations: α-Myc (Abcam), α-Flag (Sigma), α-RhoA (Santa Cruz Biotechnology), goat α-EphB2 (Santa Cruz), α-Rac1 (Millipore), α-Cdc42 (Millipore), α-β-actin (Abcam), α-PSD95 (ABR Affinity Bioreagents), α-Synapsin (Chemicon), α-HA (Santa Cruz Biotechnology), α-panphosphotyrosine 4G10 (Millipore), α-ubiquitin (Biomol International), and α-E6AP (Ube3A) (Biomol).

Mice, Cell Culture, Transfections, and Ephrin Stimulations

Ube3A$^{m-/p+}$ mice were obtained from The Jackson Laboratory, strain 129- *Ube3a*^{tm1Alb}/J, from stock number 004477. 293T cells were cultured in DMEM supplemented with 10% fetal bovine serum, 2 mM glutamine (Sigma), and penicillin/streptomycin (100 U/mL and 100 μg/mL, respectively; Sigma). Rat hippocampal neurons were prepared from E18 Long-Evans rat embryos (Charles River) as previously described (Xia et al., 1996). Mouse hippocampal neurons were prepared from E16 C57/B6 mouse embryos as previously described (Tolias et al., 2005). Hippocampal neurons were maintained in Neurobasal Medium (Invitrogen) supplemented with 2% B27 (Invitrogen), penicillin/streptomycin (100 U/mL and 100 μg/mL, respectively), and 2 mM glutamine. For synapse assays using immunofluorescence staining, hippocampal neurons were plated on glia isolated as previously described (Flavell et al., 2006). Organotypic hippocampal slice cultures were prepared from P6 E5 conditional mice as previously described (Stoppini et al., 1991). Slices were biolistically transfected with a Helios Gene Gun (Biorad) after 2 days. Bullets for the gene gun were 1.6-μm gold particles coated with 15 μg eGFP and 30 μg Cre. Empty vector plasmid was added to bring the total DNA to 60 μg in each case. Cultures were fixed, stained, and quantified for spine number at DIV6. 293T cells were transfected for 24 or 48 hr using the calcium phosphate method as previously described (Lois et al., 2002). Dissociated neurons were transfected using the Lipofectamine method (Invitrogen) according to the manufacturer's suggestions. For Ephrin stimulations in dissociated cultured neurons, mouse EB1-FC (1 μg/μL; R & D Systems) was preclustered with goat anti-human IgG FC (1.3 μg/μL; Jackson Immunoresearch) at room temperature in 1x PBS in a 1:3 ratio prior to stimulation. Preclustered EB1-FC was added to Neurobasal/B27 medium at 5 μg/mL and applied to cultured neurons. For controls, clustered goat anti-human IgG FC in Neurobasal/B27 was applied to neurons.

Cell Lysis, Immunoprecipitations, GEF Pull-Down Assays, and Western Blots

Whole rat or mouse brains or cultured cells were collected and dounce homogenized in RIPA buffer (50 mM Tris pH 8.0, 150 mM NaCl, 1% Triton X-100, 0.5% Sodium Deoxycholate, 0.1% SDS, 5 mM EDTA, 10 mM NaF, complete protease inhibitor cocktail tablet (Roche), 1 mM sodium orthovanadate, 1 mM β-glycerophosphate). For time course studies, hippocampus was freshly dissected out of whole brain and homogenized as described above. For RBD and PBD pull-down assays 293T cells were grown to ~60% confluence, transfected with plasmids for 48 hr, lysed in Mg^{2+}/lysis buffer (25 mM HEPES pH 7.5, 125 mM NaCl, 1% NP-40, 10 mM $MgCl_2$,

1mM EDTA, and 10% glycerol supplemented with complete protease inhibitor tablets from Roche), and incubated with either RBD or PBD agarose for 45 min at 4 degrees. For western blots, samples were boiled for 5 min in SDS sample buffer, resolved by SDS PAGE, transferred to nitrocellulose, and immunoblotted.

In Situ Hybridization

Probe sizes were checked by running nonhydrolyzed and hydrolyzed probes on a 1% formaldehyde agarose gel. In situ hybridization was performed as previously described (Schaeren-Wiemers and Gerfin-Moser, 1993). Briefly, P10 whole brains were embedded in Tissue-Tec and kept at −20°C. Tissue sections 14 μm-thick were sectioned onto Superfrost Plus Slides (Merck), fixed for 10 min with 4% paraformaldehyde in PBS, and subsequently washed 3 times in PBS. Acetylation of tissue sections was performed for 10 min with constant stirring in glass staining jars, and subsequently washed 3x with PBS. Slides were incubated with prehybridization solution (50% formamide, 5x SSC, 5x Denhardts solution (Sigma), Yeast tRNA) at room temperature for 6 hr to overnight. DIG-labeled probes were hydrolyzed in an alkaline hydrolysis buffer as previously described (Schaeren-Wiemers and Gerfin-Moser, 1993). Probes were diluted in prehybridization buffer at a concentration of 200 ng/mL and denatured for 5 min at 85°C prior to hybridization. Slides were incubated in 100 μL, covered by plastic coverslips (Invitrogen), and hybridization was performed overnight at 72°C. Color reaction was performed as previously described (Schaeren-Wiemers and Gerfin-Moser, 1993), except a BCIP/NBT mixture (Roche) was used according to manufacturer's instructions. Slides were mounted in *Slowfade* Gold antifade reagent with DAPI (Invitrogen) and covered with Glass Coverslides (Fisher). Sections were imaged using a Zeiss Imager.Z1 microscope with a Photometrics CoolSNAP HQ2 camera on a PLAN APO 63x/1.4 objective.

Immunocytochemistry

Neurons were fixed for 8 min at 25°C with 4% paraformaldehyde/4% sucrose in PBS. For synapse density measurement, fixed neurons were incubated with α-PSD-95 and α-Synapsin antibodies (1:200 each) in 1 × GDB (30 mM phosphate buffer [pH 7.4] containing 0.2% gelatin, 0.3% Triton X-100, and 0.8 M NaCl) overnight at 4°C. Goat α-mouse Cy3 and goat α-rabbit Cy5 (1:200 each in 1 × GDB for 1 hr at 25°C) antibodies were used to visualize the primary antibodies. For protein colocalization experiments fixed neurons were similarly treated using α-EphB2 antibodies raised in goat (1:200) and the rabbit anti-N-terminal E5 antibodies (1:200) or α-pY361-E5. For overexpression studies, transfected neurons were fixed and stained as described above using α-Myc and α-N-terminal E5 antibodies to visualize overexpressed E5 protein in the context of the GFP-labeled neurons to visualize the localization of E5 protein. Samples on coverslips were mounted on glass slides using Fluoromount-G (Southern Biotech).

Synapse Assay, Image Analysis, and Quantification

Our method for introducing shRNAs results in the transfection of a low percentage of the neurons, thus facilitating quantification of the number of synapses/dendritic spines that are present on the transfected neuron (Paradis et al., 2007). The number of dendritic spines that are present on a shRNA-expressing neuron was quantified by first marking each dendritic spine found on the developing dendrites of the transfected neuron and then using MetaMorph analysis tools to tally the number of marked spines that were present on a given length of dendrite. The number of excitatory synapses that are present on a shRNA-expressing neuron was determined by staining with the postsynaptic excitatory synaptic marker PSD-95 and the presynaptic excitatory synaptic marker Synapsin. Using MetaMorph analysis tools, we quantified the number of overlapping pre- and postsynaptic puncta on the transfected green fluorescing neuron to determine excitatory synapse density.

For dissociated neurons, images were obtained using a Zeiss Pascal confocal microscope, using a 63 × objective with sequential acquisition settings at 1024 × 1024 pixel resolution. Images for the colocalization analysis were taken with the same exposure parameters. On average, 5 stacks at 0.5 μm were taken for each neuron image. Images were collected from 10 to 15 neurons per coverslip, with two coverslips required for each condition. Synapse density was measured using Metamorph software as previously described (Universal Imaging Corporation) (Paradis et al., 2007). Because synapse density and immunostaining vary significantly between experiments, it was necessary to normalize each experiment before combining the data from individual experiments. Normalization and error propagation were performed as previously described (Paradis et al., 2007). The number of overlapping red and blue puncta greater than 2 pixels in size and localized to the transfected neuron was divided by the total dendritic area being measured. For E5 levels, the total intensity of E5 puncta over the area of the neuron was used to determine the density of E5 expression in the neuron. Statistical significance was determined by Student's t test.

For dendritic spine assays, a z series projection of each neuron was made using approximately six sections (0.45 μm/section), each averaged four times. To measure spine density, an experimenter blinded to the condition measured at least three dendritic segments totaling at least 200 μm of dendritic length/neuron, and the number of spines was counted. Between eight and ten transfected neurons were chosen randomly for quantification per experiment, and several pairs of littermates were quantified individually. For quantification of spine size, images blinded to the experimenter were analyzed using Metamorph (Universal Imaging Corporation) by manually tracing the length for at least 1000 spines per animal (Pak et al., 2001). Statistical significance was calculated using Student's t test or ANOVA.

For densitometry measurements we analyzed Western blots in the linear range using ImageJ. Each western lane is normalized to loading controls.

Array Tomography

Array tomography was performed as described previously (Micheva and Smith, 2007). In summary, acute hippocampal slices (300 μm thick) were fixed in 4% paraformaldehyde for 1 hr at room temperature and embedded in LR White resin using the benchtop protocol. Ribbons of between 30-50 serial 100 nm-thick sections prepared from wild-type and *E5* mutant mice were mounted side by side on subbed glass coverslips. Coverslips were immunostained with α-Synapsin1 (ms, Chemicon, 1:100) and α-PSD95 (Rb, ABR Affinity Bioreagents, 1:100) antibodies as described. Serial sections were imaged using a Zeiss Imager.Z1 microscope with a Photometrics CoolSNAP HQ2 camera on a PLAN APO 63x/1.4 objective. Tissue volumes were aligned using ImageJ (NIH) with the multistackreg plugin (Brad Busse). Reconstructed tissue volumes were cropped to include only stratum radiatum of CA1; and, three dimensional models of the synaptic puncta were built using Bitplane Imaris and analyzed using custom software to count synapses. This software computes the distance from the center of every synapsin puncta to the center of every PSD-95 puncta, and a synapse was counted if the distance between the centers was equal to or less than the sum of the radii of the two puncta plus an empirically determined scaling factor of 0.15 μm. All experiments were carried out and analyzed blinded to genotype.

Electrophysiology

Whole-cell voltage clamp recordings were obtained using an Axopatch 200B amplifier at 25°C. Rat hippocampal neurons were transfected with 250 ng of eGFP and 25 ng of shRNA to E5 or scrambled shRNA as a control. Four days after transfection, neurons were perfused with artificial cerebrospinal fluid containing 127 mM NaCl, 25 mM $NaHCO_3$, 1.25 mM Na_2HPO_4, 2.5 mM KCl, 2 mM $CaCl_2$, 1 mM $MgCl_2$, 25 mM glucose, and saturated with 95% O_2, 5% CO_2. The internal solution for mEPSC analysis contained 120 mM cesium methane sulfonate, 10 mM HEPES, 4 mM $MgCl_2$, 4 mM Na_2ATP, 0.4 mM Na_2GTP, 10 mM sodium phosphocreatine and 1 mM EGTA. Osmolarity and pH were adjusted to 300 mOsm and 7.3 with Millipore water and CsOH, respectively.

The mEPSCs were isolated by exposing neurons to 0.5 μM tetrodotoxin, 50 μM picrotoxin (Tocris Bioscience), and 10 μM cyclothiazide. Cells with series resistance larger than 25 MΩ during the recordings were discarded. Data were analyzed in IgorPro (Wavemetrics) using custom-written macros. For each trace, the event threshold was set at 1.5 times the root-mean-square current. Currents were counted as events if they crossed the event threshold, had a rapid rise time (1.5 pA ms^{-1}) and had an exponential decay ($\tau < 50$ ms for mEPSC).

Statistical significance was determined by two methods. First, 50 random points selected from each cell were concatenated to describe the cumulative distributions of events in each condition and then compared by a Kolmogorov–Smirnov test. Second, a Monte Carlo simulation was performed in which points were randomly sampled from each condition and the mean of these samples compared at least 1,000 times. $p < 0.05$ from both tests was considered significant.

SUPPLEMENTAL REFERENCES

Flavell, S.W., Cowan, C.W., Kim, T.K., Greer, P.L., Lin, Y., Paradis, S., Griffith, E.C., Hu, L.S., Chen, C., and Greenberg, M.E. (2006). Activity-dependent regulation of MEF2 transcription factors suppresses excitatory synapse number. Science *311*, 1008–1012.

Lin, Y., Bloodgood, B.L., Hauser, J.L., Lapan, A.D., Koon, A.C., Kim, T.K., Hu, L.S., Malik, A.N., and Greenberg, M.E. (2008). Activity-dependent regulation of inhibitory synapse development by Npas4. Nature *455*, 1198–1204.

Lois, C., Hong, E.J., Pease, S., Brown, E.J., and Baltimore, D. (2002). Germline transmission and tissue-specific expression of transgenes delivered by lentiviral vectors. Science *295*, 868–872.

Micheva, K.D., and Smith, S.J. (2007). Array tomography: a new tool for imaging the molecular architecture and ultrastructure of neural circuits. Neuron *55*, 25–36.

Pak, D.T., Yang, S., Rudolph-Correia, S., Kim, E., and Sheng, M. (2001). Regulation of dendritic spine morphology by SPAR, a PSD-95-associated RapGAP. Neuron *31*, 289–303.

Paradis, S., Harrar, D.B., Lin, Y., Koon, A.C., Hauser, J.L., Griffith, E.C., Zhu, L., Brass, L.F., Chen, C., and Greenberg, M.E. (2007). An RNAi-based approach identifies molecules required for glutamatergic and GABAergic synapse development. Neuron *53*, 217–232.

Schaeren-Wiemers, N., and Gerfin-Moser, A. (1993). A single protocol to detect transcripts of various types and expression levels in neural tissue and cultured cells: in situ hybridization using digoxigenin-labeled cRNA probes. Histochemistry *100*, 431–440.

Stoppini, L., Buchs, P.A., and Muller, D. (1991). A simple method for organotypic cultures of nervous tissue. J. Neurosci. Methods *37*, 173–182.

Tolias, K.F., Bikoff, J.B., Burette, A., Paradis, S., Harrar, D., Tavazoie, S., Weinberg, R.J., and Greenberg, M.E. (2005). The Rac1-GEF Tiam1 couples the NMDA receptor to the activity-dependent development of dendritic arbors and spines. Neuron *45*, 525–538.

Xia, Z., Dudek, H., Miranti, C.K., and Greenberg, M.E. (1996). Calcium influx via the NMDA receptor induces immediate early gene transcription by a MAP kinase/ERK-dependent mechanism. J. Neurosci. *16*, 5425–5436.

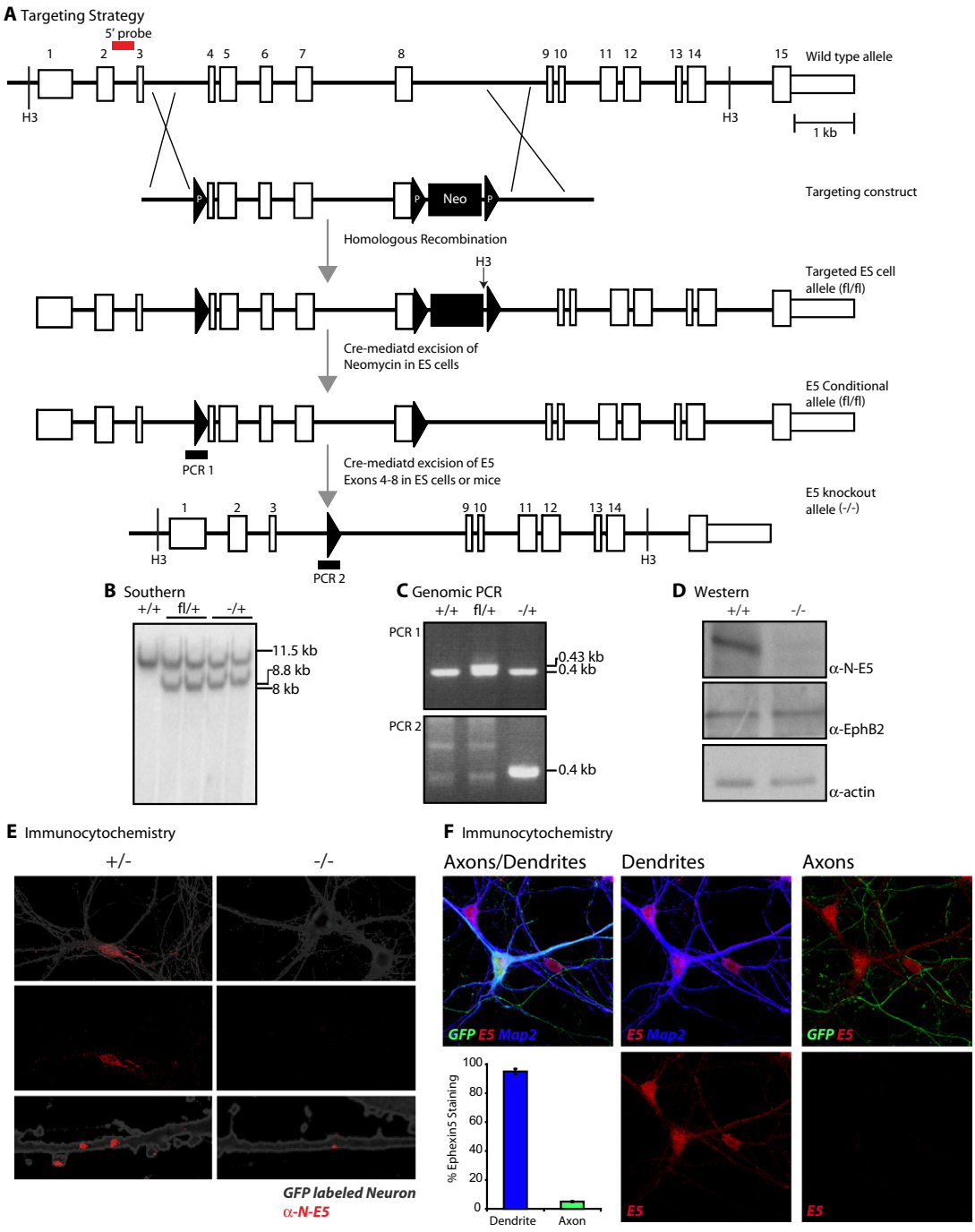

Figure S1. Construction and Validation of the *E5*$^{-/-}$ and *E5*$^{fl/fl}$ Mice, Related to Figure 1

(A) Scheme used to generate the *E5*$^{-/-}$ and *E5*$^{fl/fl}$ mice. The middle five exons (shown numbered) were flanked with loxP sites (triangles with the letter "P"). The neomycin resistance gene (Neo) was removed by the expression of Cre-recombinase to generate an E5 conditional allele (fl/fl). The remaining loxP sites were deleted by expression of Cre-recombinase to generate an E5 knockout allele (−/−). Red bars indicate location of southern probes. Thick black bars indicate location of genomic PCR primer pairs.

(B) Southern blot showing the successful removal of exons 4 through 8 in the *E5* gene in mouse ES cells. Genomic DNA was digested with HindIII and hybridized with a 5′ probe shown in A).

(C) PCR analysis of genomic tail DNA showing that the *E5* gene is correctly targeted, compared to wild-type (+/+) recombined in *E5*$^{-/+}$ (-/+) and *E5*$^{fl/+}$ (fl/+) mice. PCR 1 is using primers which flank the first loxP site (top). A 0.4 kb band is expected for wild-type and 0.43 is expected for loxP insertion. PCR 2 is using primers which flank the first and second loxP site (bottom). No band is expected in a wild-type or nonrecombined floxed. A 0.4 kb band is expected for a completely recombined knockout.

(D) Whole brain lysates from wild-type (+/+) mice of indicated ages were assessed for E5 protein expression by immunoblot with α-N-E5 (top). Western blot showing that E5 protein is absent in $E5^{-/-}$ (−/−) mice. α-EphB2 and α-Actin serve as a loading control.

(E) Immunocytochemistry of dissociated cultures from $E5^{+/-}$ (+/−) and $E5^{-/-}$ (−/−) mice using α-N-E5 antibody reveals specific staining of E5 along the dendrite of the developing neuron, near dendritic spines, and within the soma. Magnified images show dendrites of stained neurons.

(F) E5 is expressed exclusively in the dendrite of the developing hippocampus. Cultured hippocampal neurons were transfected with GFP (Green) at DIV8 and fixed and stained two days later for endogenous E5 expression (red) and the dendritic marker Map2 (Blue). Overlapped Map2/GFP staining indicates the dendrites of the transfected neuron (Top/Middle panel). Conversely, subtraction of Map2-positive processes from GFP-labeled neuronal staining indicates location of axons on the transfected neuron (Top/Right). To determine localization of E5 staining, the percent of E5 puncta on GFP labeled dendrites were compared to the percent of E5 puncta on GFP labeled axons. Quantification was done using MetaMorph. Almost no staining of E5 was observed along axons.

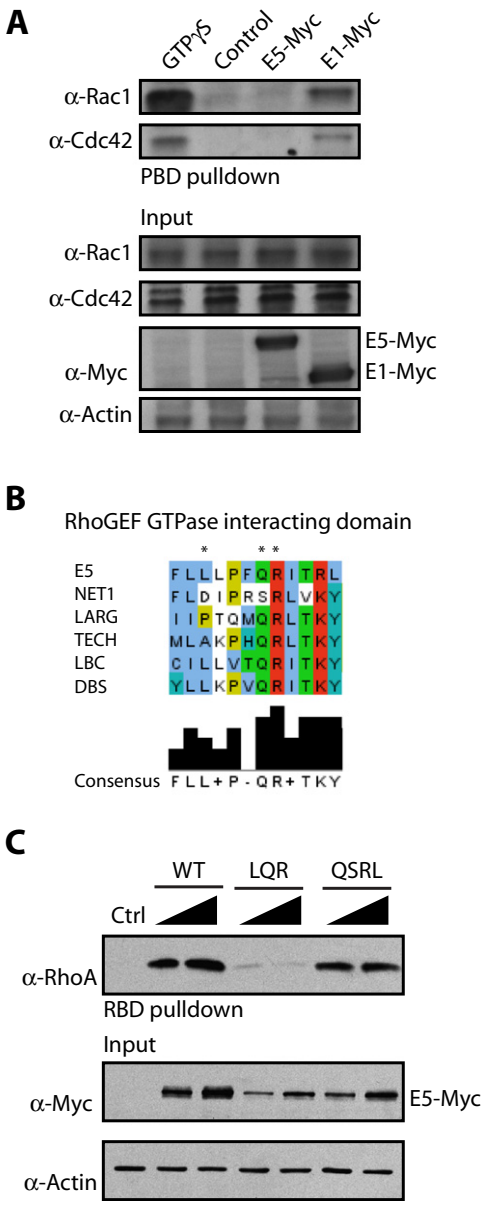

Figure S2. Ephexin5 GEF Domain Analysis, Related to Figure 2

(A) Lysates from 293 cells previously transfected with empty vector (Control), E5-Myc, or E1-Myc were assayed for activated Rac1 and Cdc42 using the PBD pull-down assay. Pull-down lanes were immunoblotted with mouse anti-Rac1 and reprobed with rabbit anti-Cdc42 (top two panels). GTPγS lane is a positive control for inducing Rac1 and Cdc42 activity. Increased endogenous Rac1 or Cdc42 activity is demonstrated by presence of α-Rac1 or α-Cdc42 signal in PBD pull-down lanes. Input protein levels and α-Actin loading control are shown (Bottom).

(B) Sequence alignment of the α5 helix loop of the E5-DH domain to known RhoA-specific GEFs. Asterisks highlight residues important for GEF activity.

(C) Lysates from 293T cells previously transfected with empty vector, E5-Myc (WT), E5-LQR-Myc (LQR), or E5-QSRL-Myc (QSRL) were assayed for activated RhoA using RBD pull-down assay as previously described. Total protein levels were assessed by immunoblotting for α-Myc and α-Actin (Input panels).

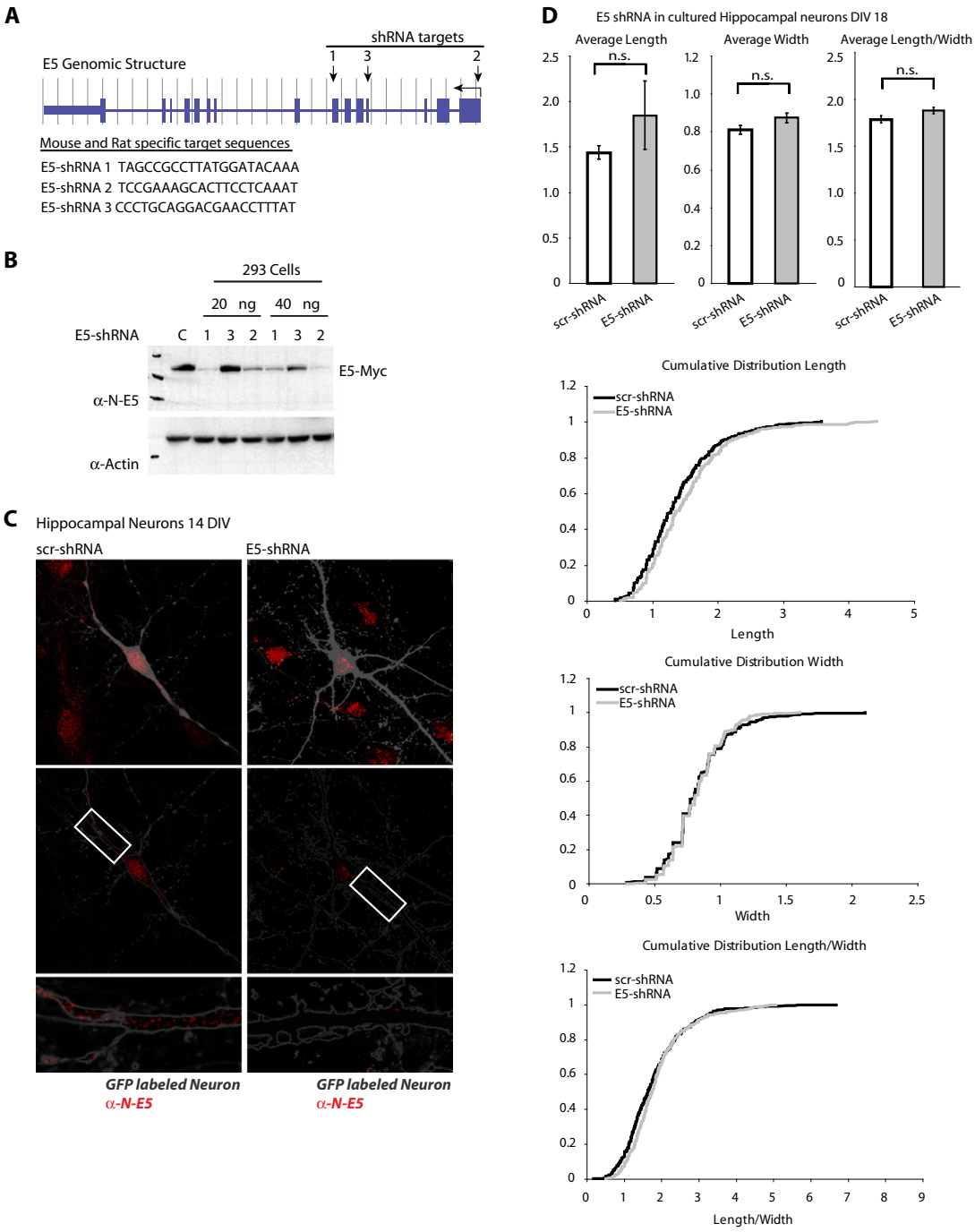

Figure S3. Ephexin5 Knockdown by shRNA, Related to Figure 3

(A) Genomic structure of the *E5* gene. Arrows indicate sites of shRNA targeting. The shRNA sequences used for E5 knockdown are shown.

(B) Lysates from 293 cells previously transfected with E5-Myc alone (C) or together with E5-shRNA at two different concentrations (20 ng or 40 ng) were run on SDS-PAGE and immunoblotted with α-N-E5 antibody. Western blot showing that exogenously expressed E5 protein can be knocked down in 293T cells in the presence of shRNA constructs. Only two of the three shRNA constructs were capable of knocking down E5 protein expression. Actin loading controls are shown using α-Actin antibodies (bottom).

(C) Rat hippocampal neurons were transfected with GFP (Gray) and scrambled control shRNA (scr-shRNA) or E5 targeting shRNA (E5-shRNA) at DIV10. At DIV14, neurons were fixed and stained for endogenous E5 protein using α-N-E5 antibody. Immunocytochemistry shows that E5 shRNA-expressing neurons have a dramatic decrease in endogenously expressed E5 especially along dendrites. White rectangle outlines magnified dendritic region showing E5 staining in bottom panel.

(D) Loss of E5 function does not affect dendritic spine morphology. 10 ng of E5 shRNA (E5-shRNA) or scrambled shRNA (scr-shRNA) was cotransfected with GFP

into rat hippocampal neurons at DIV14. At DIV18, transfected neurons were fixed and spines quantified for spine length and head width. Data are plotted as cumulative distribution to identify populations of spines that have changed in length or width. All error bars are SEM; *p < 0.002.

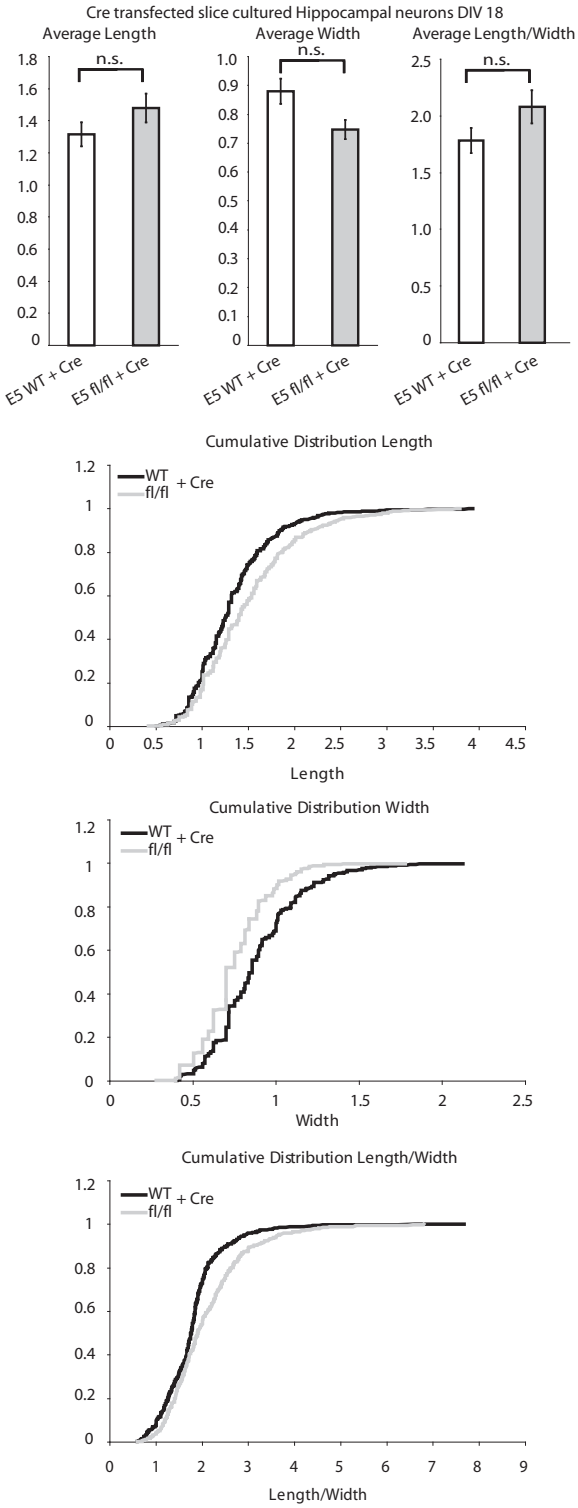

Figure S4. Effect of Ephexin 5 Knockdown on Spine Length and Width, Related to Figure 4

Loss of E5 function does not affect dendritic spine morphology in an intact circuit. Organotypic slices were prepared from P7 WT and E5 conditional littermates and at DIV3 biolistically transfected with Cre or control plasmid and GFP. At DIV7 (analogous to DIV14 in dissociated cultures) neurons were fixed and mounted for imaging. Over 200 μm of dendrite was imaged per neuron with 10 neurons imaged per animal totaling over 3000 spines. The data represent at least two animals from a total of two different litter pairs quantified at the same time. These results were verified by blinded counting and quantification from a third party to verify significance. Data are plotted as cumulative distribution to identify populations of spines that have changed in length or width.

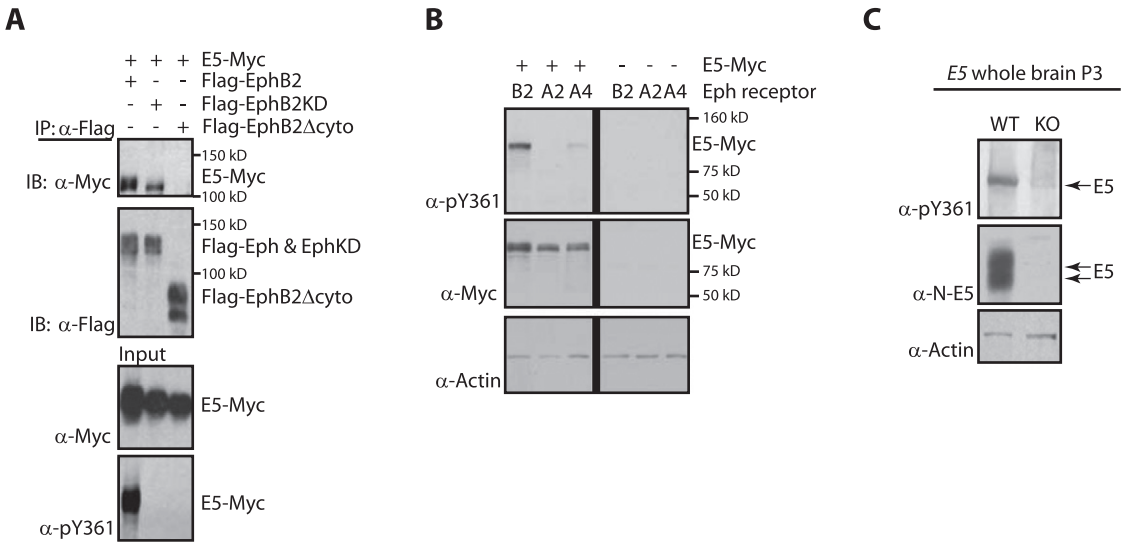

Figure S5. EphB Mediates Phosphorylation of Ephexin5 at Tyrosine-361, Related to Figure 5

(A) Both the EphB2 cytoplasmic domain and kinase domain are necessary for E5 phosphorylation, but only the EphB2 cytoplasmic domain is required for the EphB2 interaction with E5. 293T cell lysates from transfected cells with E5-Myc with either Flag-EphB2, Flag-EphB2-kinase dead (KD), or Flag-EphB2-Δcyto were immunoprecipitated with α-Flag antibody followed by immunoblotting with α-Flag or with α-Myc antibodies to assay for immunoprecipitated Ephs and E5, respectively. Input cell lysates were immunoblotted with α-Myc and α-pY361. Time of transfection was kept short and with high ratio of Ephexin5 to EphB to limit EphB-dependent degradation of Ephexin5.

(B) E5 is preferentially phosphorylated by EphB2. 293T cell lysates from cells previously transfected with the indicated Ephs, with or without E5-Myc were immunoblotted with antibodies to α-pY361, α-Myc, and α-Actin.

(C) E5 is phosphorylated in mouse brain at tyrosine 361. Whole brain lysates from P3 wild-type (WT) and *E5*$^{-/-}$ (KO) littermates were lysed and immunoblotted with α-pY361, α-E5 (α-N-E5) and α-β-Actin.

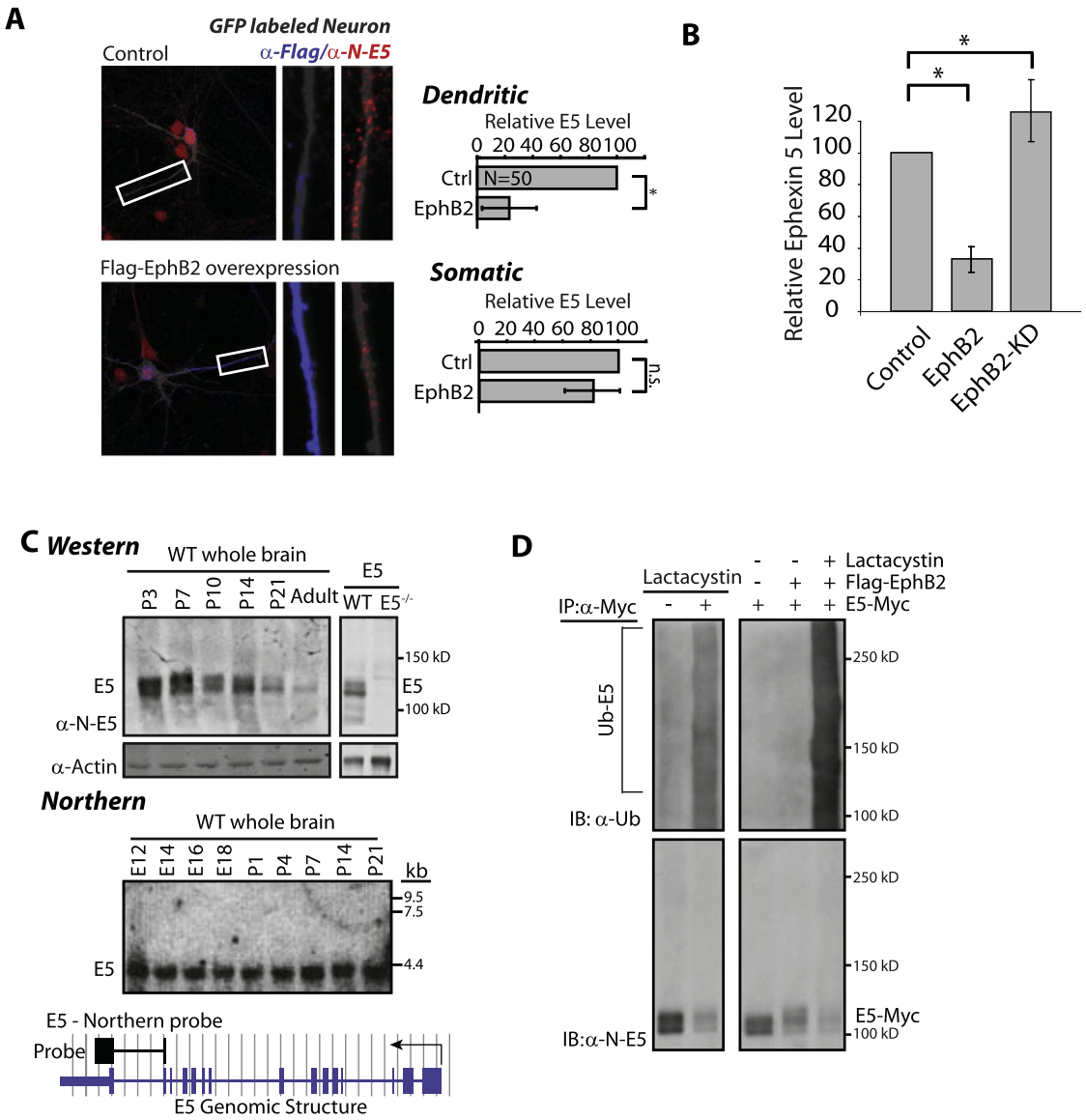

Figure S6. EphB2-Mediated Degradation of Ephexin5 Is Kinase- and Proteasome Dependent, Related to Figure 6

(A) Dissociated mouse hippocampal neurons were cotransfected at DIV10 with GFP (gray) and plasmid containing EphB2-Flag. At DIV14 neurons were fixed and stained for endogenous E5 (α-N-E5, Red) or EphB2-Flag (α-Flag, Blue). Representative images show transfected neurons (left). White rectangle outlines magnified dendritic region showing examples of EphB2 or E5 staining (right). Three independent experiments were quantified for dendritic and somatic endogenous E5 as described in methods (right). Error bars ± SEM; *p < 0.05.

(B) Dissociated mouse hippocampal neurons were cotransfected at DIV10 with GFP (gray) and plasmid containing EphB2-Flag or EphB2-KD-Flag. At DIV14 neurons were fixed and stained for endogenous E5 similar to panel (A). Three independent experiments were quantified for dendritic and somatic endogenous E5 as described in methods (right). Error bars ± SEM; *p < 0.05.

(C) Whole brain lysates from wild-type mice of indicated ages were assessed for E5 protein expression by immunoblot with α-N-E5 (top). Immunoblot of brain lysates from WT and $E5^{-/-}$ mice is shown. α-Actin was used as loading control. Levels of E5 RNA from wild-type mice of indicated ages were assessed by northern analysis using an E5 specific probe. Schematic of *E5* genomic locus shows location of northern probe (Bottom).

(D) 293 cells transfected with E5-Myc were treated with vehicle control (-) or proteasome inhibitor lactacystin (+). Lysates from transfected 293 cells were immunoprecipitated with α-Myc, followed by immunoblotting with α-N-E5 or ubiquitin (α-ub) (left). Similar experiment was repeated in the presence or absence of cotransfected Flag-EphB2 (right).

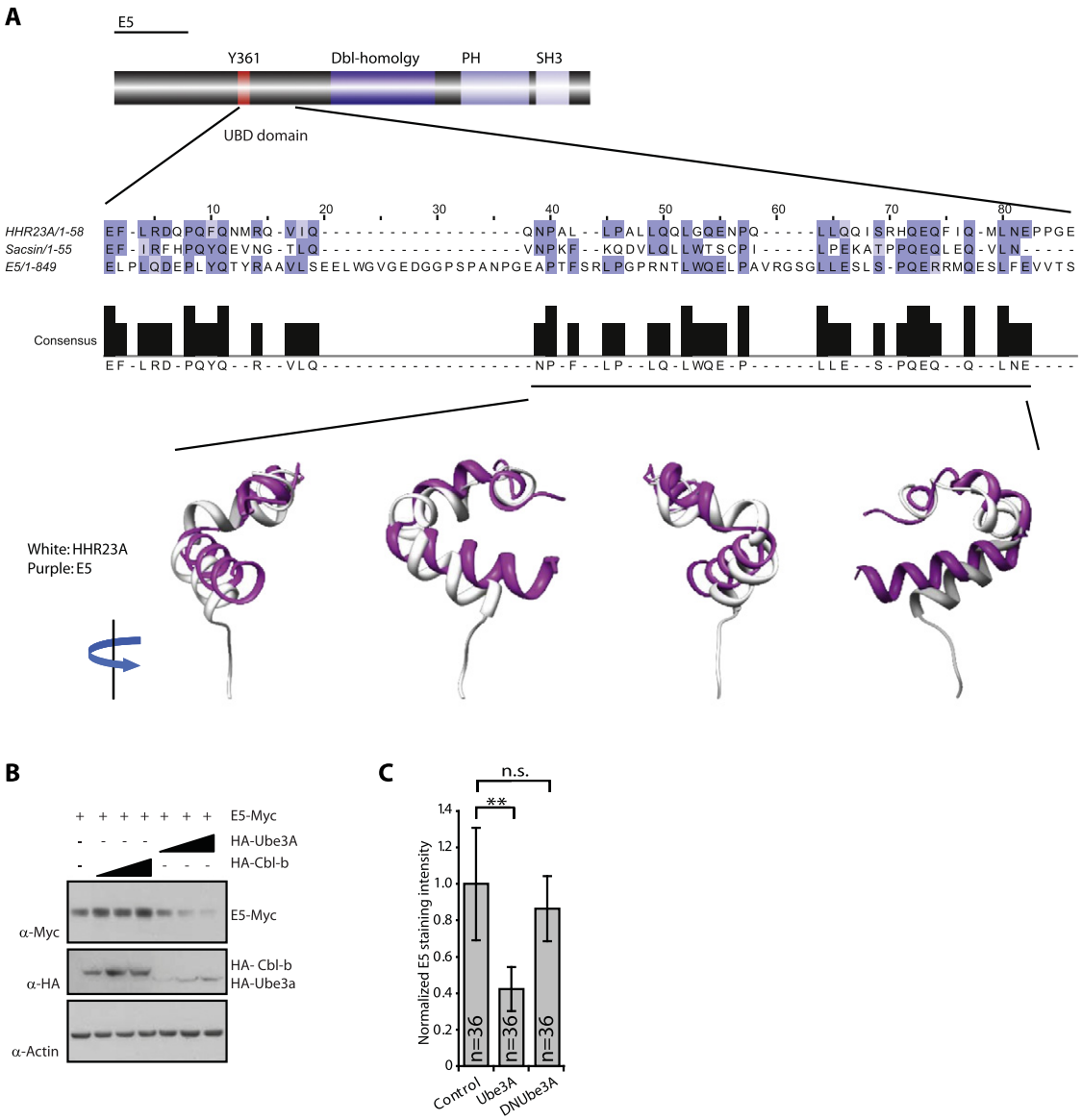

Figure S7. Ephexin5 UBD and Degradation by Ube3A, Related to Figure 7

(A) Schematic of E5 showing Dbl-homology domain (dark blue), PH domain (light blue), SH3 domain (white), and Y361 phosphorylation site (red). Expanded sequence is at location of predicted Ube3A binding domain (UBD). Predicted UBD sequence of E5 is aligned with known UBD containing proteins HHR23A and Sacsin (Greer et al., 2010) using ClustalW (http://www.ebi.ac.uk/Tools/clustalw2/index.html). Underlined protein sequence was modeled for E5 and HHR23A and overlaid using ModBase (http://modbase.compbio.ucsf.edu/modbase-cgi/search_form.cgi).

(B) Lysates from 293 cells previously transfected with various combinations of plasmids containing E5-Myc, HA-Ube3A and/or HA-Cbl-b were immunoblotted with α-Myc, α-HA, or α-Actin (loading control).

(C) Hippocampal mouse neurons were cotransfected with GFP and control, HA-Ube3A or HA-DNUbe3A at DIV10. At DIV14 Neurons were fixed and stained for E5 and quantified according to methods. Quantification is of E5 staining intensity normalized to control. Error bars ± SEM; **p < 0.01, ANOVA.